4

Results

4.1 Biochemical changes in the tea plant in response to TMB-herbivory

4.1.1 Total phenolic content

The total phenolic content of the tea tissues (two leaves and a bud) was found to be reduced in the infested samples of all of the clones studied. However, none of the infested clones exhibited significant decrease in total phenolic content when compared with the non-infested healthy ones. Overall, the total phenolic content was found to be much higher in the Darjeeling clones i.e., P312 and AV2.

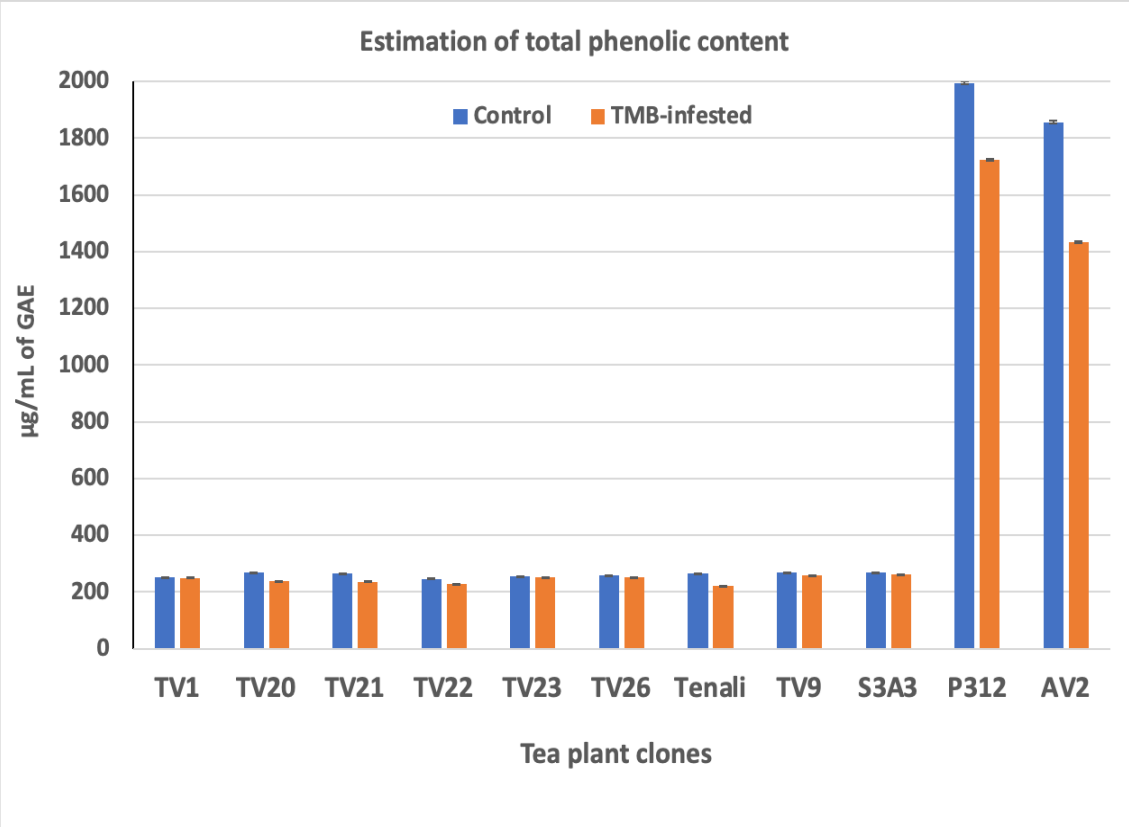

Fig. 4.1 Total phenolic content in 11 clones of tea plant. (Data is represented as mean ± SE, n = 3). Statistical significance was calculated through a one-way ANOVA. P-value ≤ 0.05 was used as the significance value.

4.1.2 Total flavonoid content

The infested tea plants exhibited higher total flavonoid content than the healthy plants in all of the clones studied. This increase in total flavonoid content is found to be significant in all of the clones. Higher flavonoid content in response to TMB herbivory might attribute to the purpose of flavonoids as defense secondary metabolites that have insect repellent and insect toxic properties.

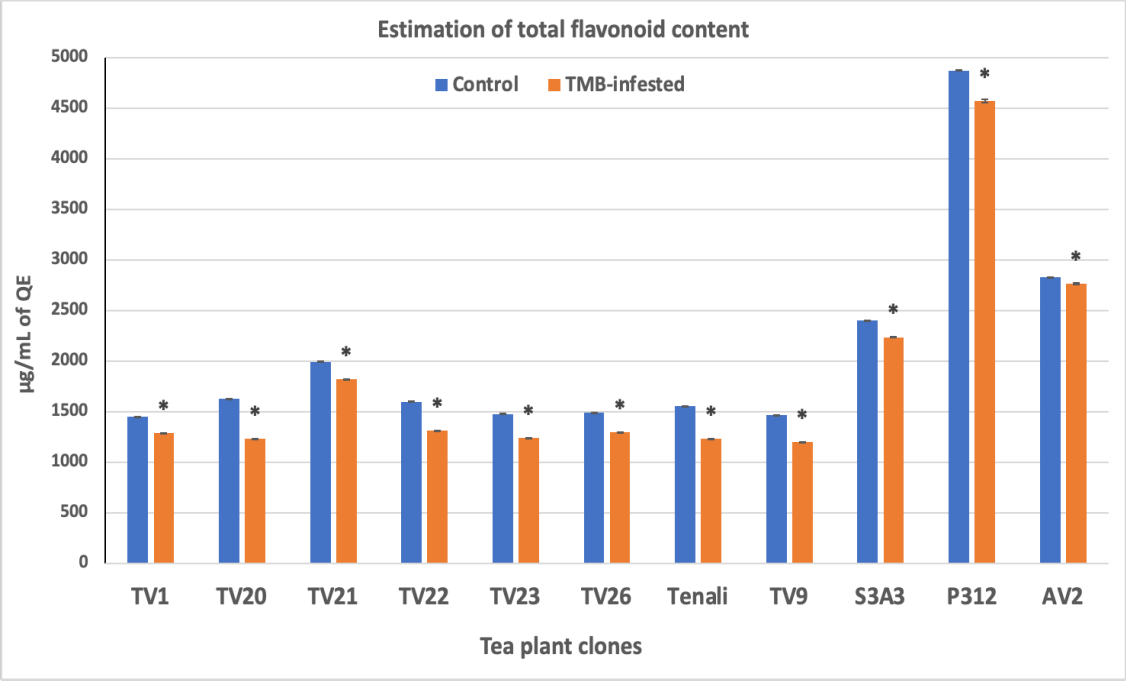

Fig. 4.2 Total flavonoid content in 11 clones of tea plant. (Data is represented as mean ± SE, n = 3). Statistical significance was calculated through a one-way ANOVA followed by a post-hoc t-test with Bonferroni's correction method. P-value ≤ 0.05 was used as the significance value. Statistically significant data are represented with *.

4.1.3 Enzymatic antioxidants

We determined the enzymatic antioxidant activities of the tea plants and compared the enzymatic activities of infested tissues with the non-infested tissues. In general, POX, APX, PAL, PPO and CAT activities were influenced by TMB herbivory in the plant.

4.1.3.1 Peroxidase (POX) activity

The activity of POX was significantly increased in response to TMB feeding in all of the studied tea plant clones. POX activity was seen to be highest in TV1 relative to the other clones. TV20 and Tenali showed lesser POX activity in general.

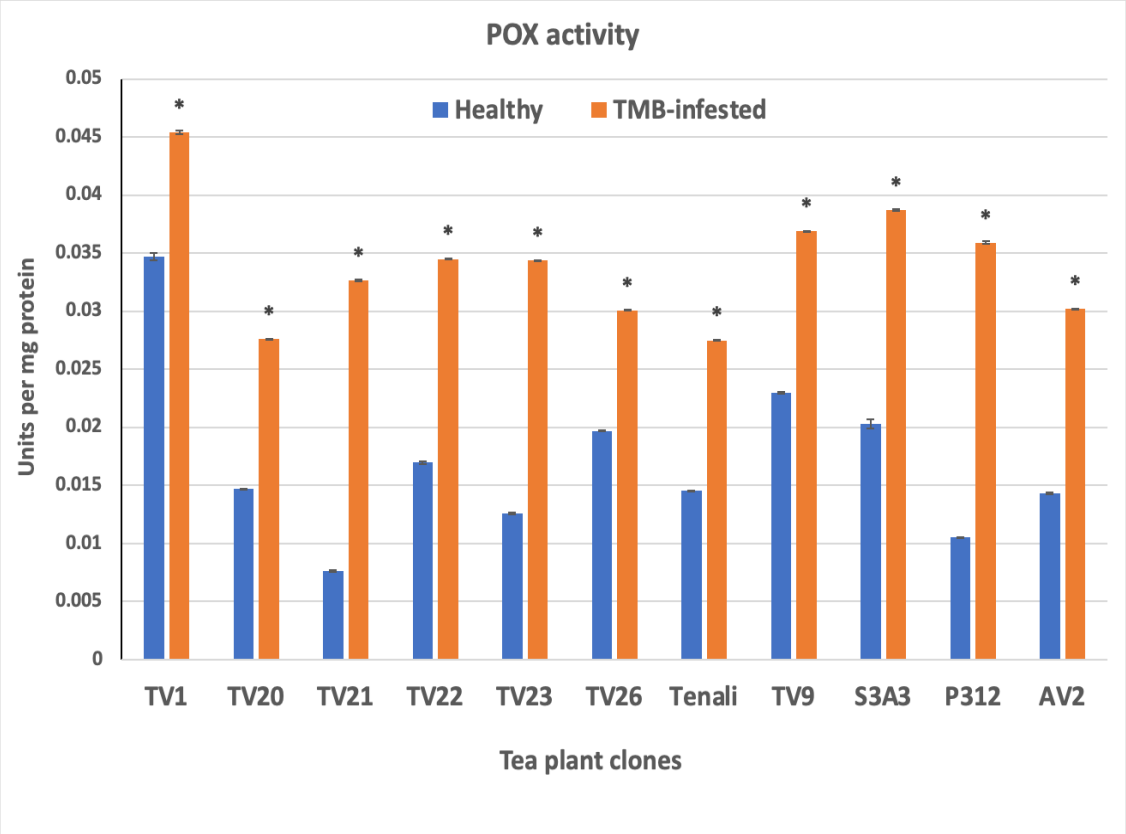

Fig. 4.3 POX activity in 11 clones of tea plant. (Data is represented as mean ± SE, n = 3). Statistical significance was calculated through a one-way ANOVA followed by a post-hoc t-test with Bonferroni's correction method. P-value ≤ 0.05 was used as the significance value. Statistically significant data are represented with *.

4.1.3.2 Ascorbate peroxidase (APX) activity

TMB feeding influenced a tremendous increase in APX activity of the tea plants infested by TMB than the control plants. All of the clones showed significant elevation of APX

activity when infested by the insect. TV22 exhibited the highest APX activity among all the clones, while TV23 exhibited the lowest.

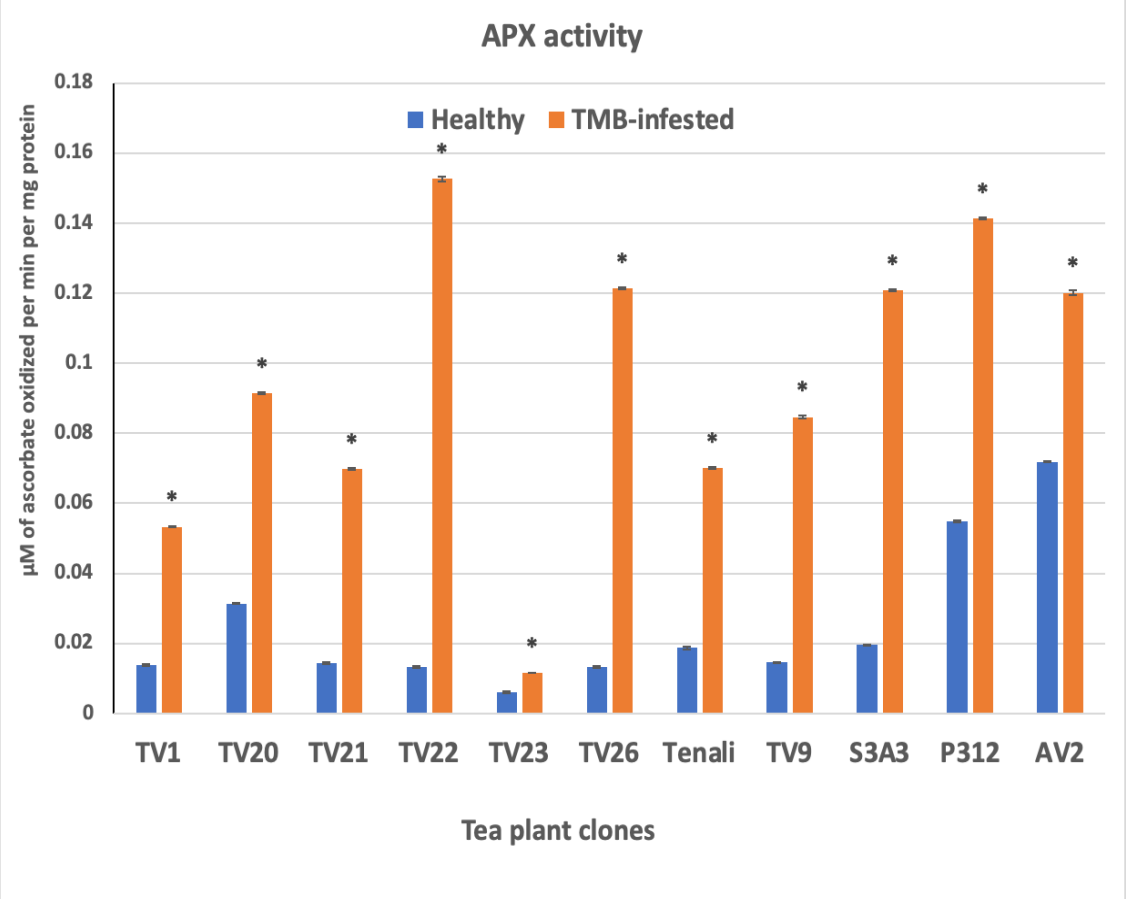

Fig. 4.4 APX activity in 11 clones of tea plant. (Data is represented as mean ± SE, n = 3). Statistical significance was calculated through a one-way ANOVA followed by a post-hoc t-test with Bonferroni's correction method. P-value ≤ 0.05 was used as the significance value. Statistically significant data are represented with *.

4.1.3.3 Phenylalanine ammonia lyase (PAL) activity

The activity of PAL was also seen to be increased in the infested plants. However, this increase was not significant in TV1 and P312, while the others showed significant increase in the enzyme activity. Clone S3A3 showed the highest PAL activity, while TV23 the lowest.

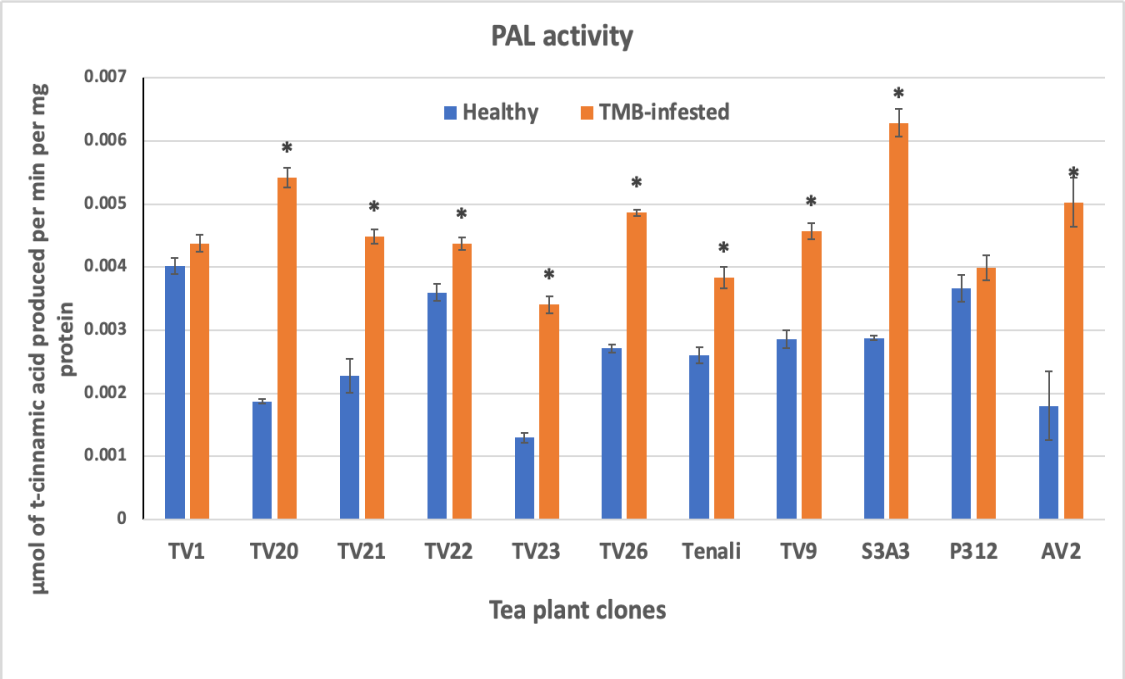

Fig. 4.5 PAL activity in 11 clones of tea plant. (Data is represented as mean ± SE, n = 3). Statistical significance was calculated through a one-way ANOVA followed by a post-hoc t-test with Bonferroni's correction method. P-value ≤ 0.05 was used as the significance value. Statistically significant data are represented with *.

4.1.3.4 Polyphenol oxidase (PPO) activity

The activity of the enzyme PPO was seen to be increased in the infested plants belonging to all clones except TV1, where it was seen to be significantly decreased. P312 exhibited the highest PPO activity among all the clones, followed by AV2, Tenali and TV21.

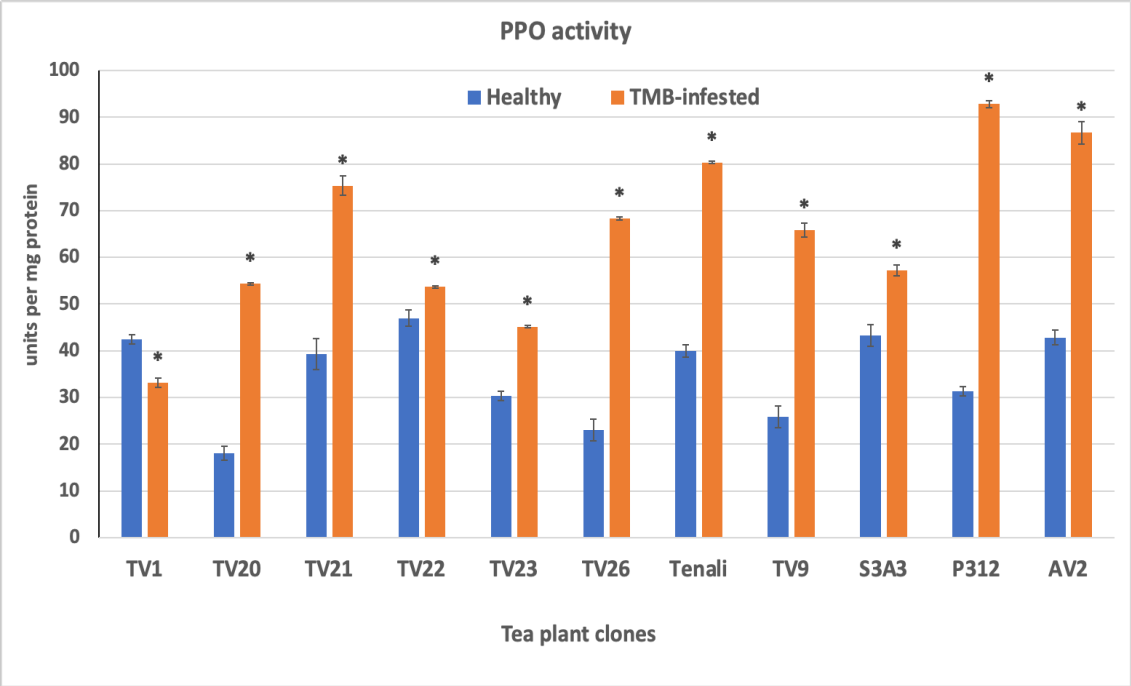

Fig. 4.6 PPO activity in 11 clones of tea plant. (Data is represented as mean ± SE, n = 3). Statistical significance was calculated through a one-way ANOVA followed by a post-hoc t-test with Bonferroni's correction method. P-value ≤ 0.05 was used as the significance value. Statistically significant data are represented with *.

4.1.3.5 Catalase (CAT) activity

TMB feeding impacted CAT enzymatic activity too. CAT activity was found to be tremendously increased in all of the infested clones. This increase in activity was noted highest in AV2, followed by P312, TV9 and TV1. All the clones showed significant elevation of CAT activity in the TMB-stressed plants.

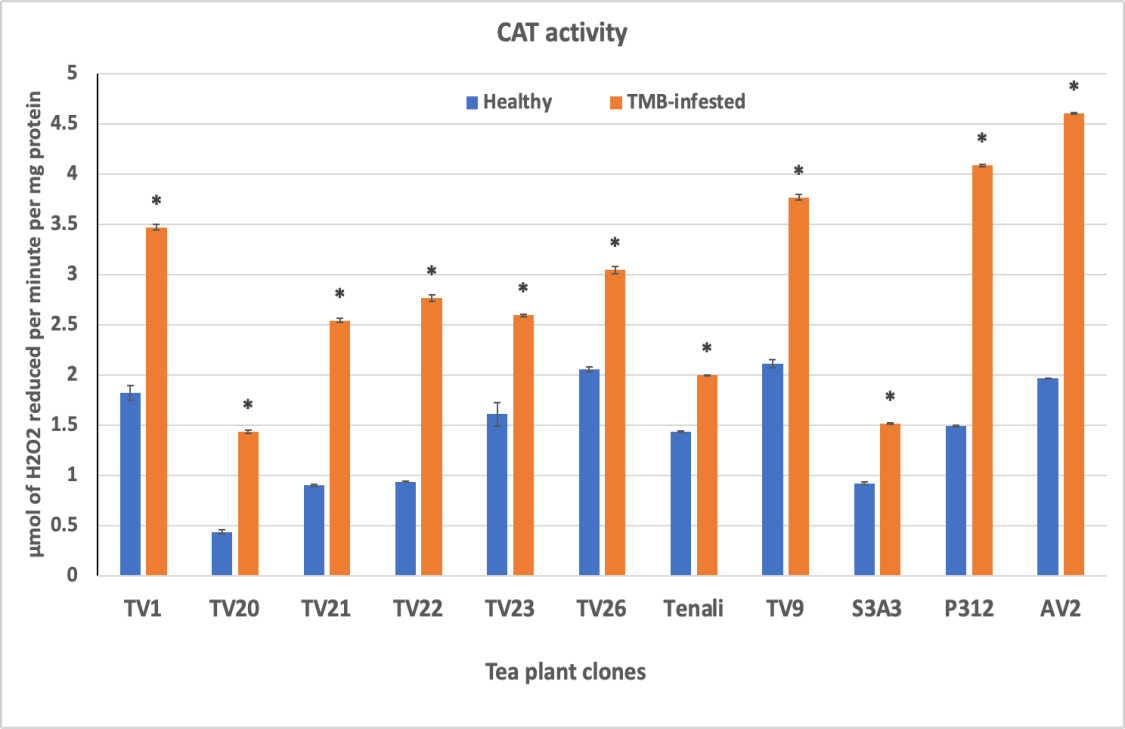

Fig. 4.7 CAT activity in 11 clones of tea plant. (Data is represented as mean ± SE, n = 3). Statistical significance was calculated through a one-way ANOVA followed by a post-hoc t-test with Bonferroni's correction method. P-value ≤ 0.05 was used as the significance value. Statistically significant data are represented with *.

4.2 Sequencing reads summary

Trimming of adapters from sequencing data and subsequent assessment of quality of the reads generated from the high-throughput sequencing showed that quality score of all six libraries (Control-1, Control-2, Control-3, Infested-1, Infested-2, Infested-3) were in range of 28-40, with 39 as the average read quality score, which is a good phred quality score for data analysis. The figures of data quality check are included in the Appendix section.

We obtained an average of 14.7 gb of clean data for each of the six libraries. The clean reads were successfully aligned to *C. sinensis* reference genome (Xia *et al*. 2020) with an average of 80.83 % alignment rate for healthy and TMB-infested RNA-seq

libraries. In total, 154463 transcripts were obtained after transcriptome assembly and reconstruction. Table 4.1 shows summary of the alignment of the six libraries.

Table 4.1 Summary of reads generated from control and TMB-infested tea samples

Sample	**Clean reads**	**Mapped reads**	**Reads mapped 0 times**	**Reads mapped exactly 1 time**	**Reads mapped > 1 time**	**GC %**
Control-1	37232696	30985049 (83.22%)	7654183	10722775	18855738	53
Control-2	46627161	38597963 (82.78%)	9964320	14226132	22436709	52
Control-3	35846318	29698674 (82.85%)	7633635	10709863	17502820	52
Infested-1	44100615	34292638 (77.76%)	11608865	12376846	20114904	52
Infested-2	46777943	36772141 (78.61%)	11834865	12784517	22158561	53
Infested-3	45820093	36550688 (79.77%)	11009782	11330617	23479694	53

4.3 LncRNAs

4.3.1 Identification of lncRNAs

The obtained 154463 transcripts underwent a series of screening for prediction of lncRNAs in the libraries. Discarding of transcripts based on class codes, number of exons, ORF length and length of nucleotides, resulted in 21017 transcripts. Of them, CPC, CNCI

and PLEK softwares predicted 1617 transcripts to have coding potential. The remaining filtered transcripts were put under stringent criteria to eliminate any of them showing sequence homology with known proteins and housekeeping RNAs. A total of 9502 transcripts were identified as putative candidate lncRNAs from control and TMB infested tissues.

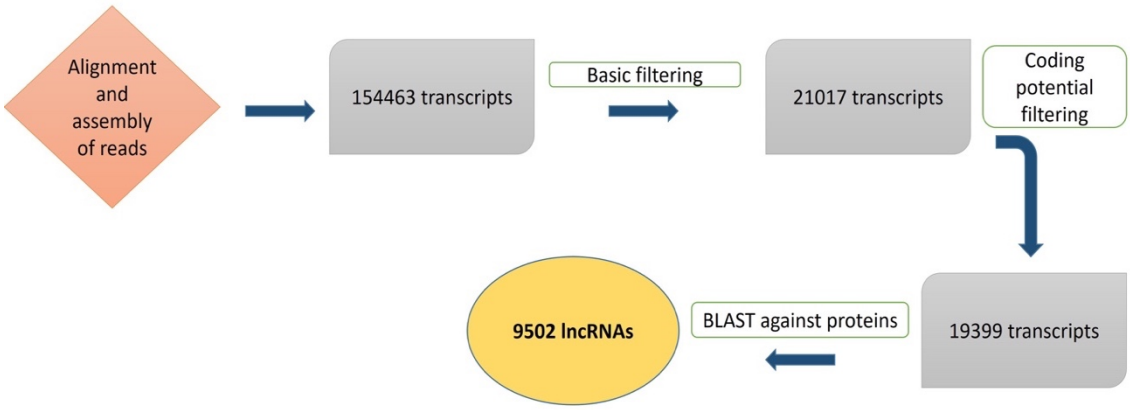

Fig. 4.8 Filtering of transcripts for identification of putative lncRNAs

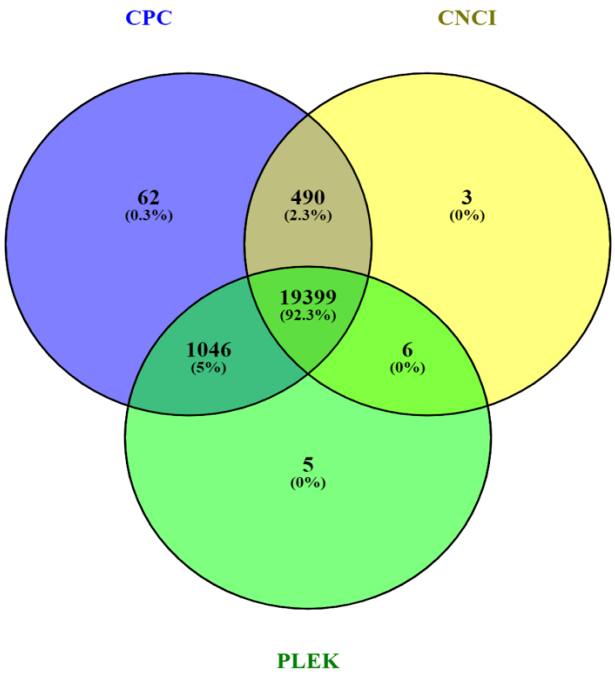

Fig. 4.9 Coding potential analysis of the assembled transcripts through three tools

4.3.2 Characterization of lncRNAs

Analysis of the chromosomal distribution of pattern of lncRNAs revealed that among the 15 chromosomes, chromosome 1 of the *C. sinensis* genome contained the most number of lncRNAs i.e., 733.

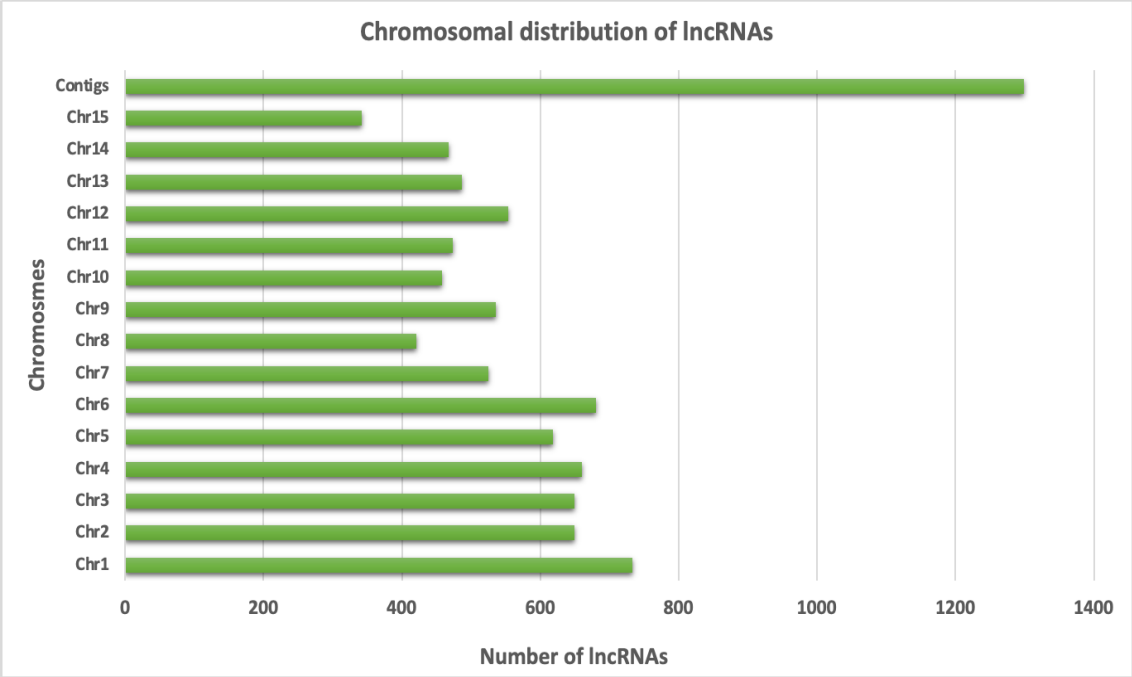

Fig. 4.10 Chromosomal distribution of identified lncRNAs

Based on their genomic positions, the predicted lncRNAs were subdivided into various classes. Majority of the lncRNAs (70.56%) were found to be lincRNAs i.e., they originated from intergenic/unknown regions of the genome (class code "u"), the second most abundant class of lncRNAs (17.35%) was intronic lncRNAs (incRNAs) that were predicted from introns of coding genes (class code "i") followed by sense lncRNAs (9.5%) that exhibited exonic overlaps (class code "o") and the least abundant group of lncRNAs (2.56%) was antisense lncRNAs (lncNATs) that were identified from antisense strand of coding genes (class code "x").

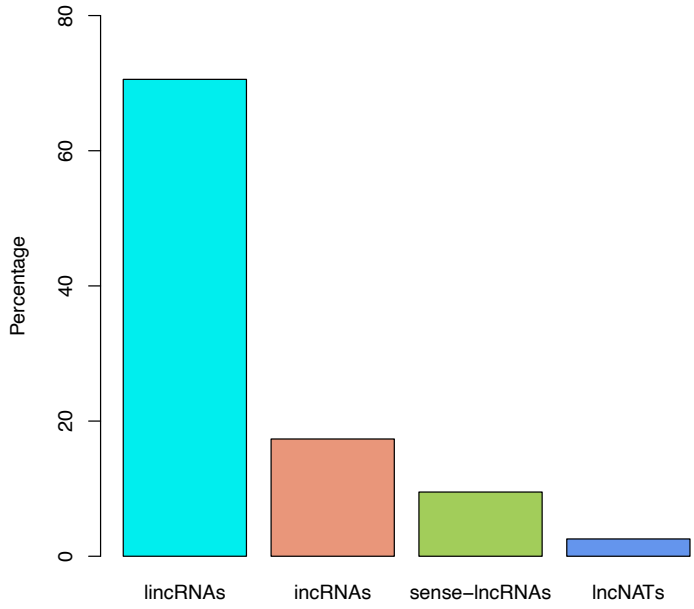

Fig. 4.11 Classification of identified lncRNAs based on their genomic position

To understand sequence conservation and similarity among plant lncRNAs, we conducted a conservation analysis of the identified lncRNAs by running a BLAST search against lncRNAs of several plant species deposited in CANTATAdb (Szcześniak *et al*. 2019), GreeNC (Gallart *et al*. 2016) and NONCODE (Liu *et al*. 2005) databases. In total, only 82 lncRNAs (0.86%) identified in this study were homologous with lncRNAs of 34 plant species implying that *C. sinensis* lncRNAs are poorly conserved among those of other plant species. Majority of the BLAST hits was recorded from lncRNAs of *Triticum aestivum* (12.36%) followed by those of *Medicago truncatula* (9.74%), *Chenopodium quinoa* (9.21%), *Brassica napus* (8.16%) and *Vitis vinifera* (8.16%).

The length distribution and exon numbers of lncRNAs illustrated that most of the lncRNAs (62.14%) were found to be < 400 nucleotides in length and only a few of them (4.58%) were longer than 1000 bp. The average length of the lncRNAs was 432 nucleotides. The lncRNAs exhibited exon numbers in a range of 2-8 where 83.6% comprised of two exons and only 0.01% had eight exons (Fig. 4.12).

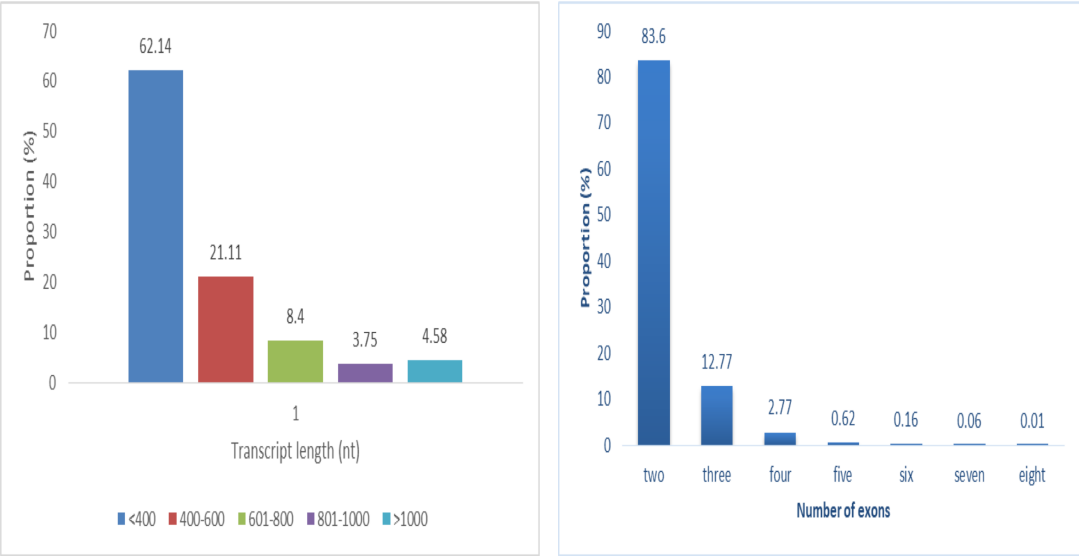

Fig. 4.12 Length distribution and number of exons found in the identified lncRNAs

4.3.3 Expression of lncRNAs

Out of 9502 lncRNAs, 6703 lncRNAs were expressed in healthy and infested tissues, 1656 lncRNAs were selectively expressed in healthy tissues and 1142 lncRNAs were specific to TMB infested tissues (Fig. 4.13) The FPKM values of expression levels of identified lncRNAs in the six samples has been shown in Fig 4.14.

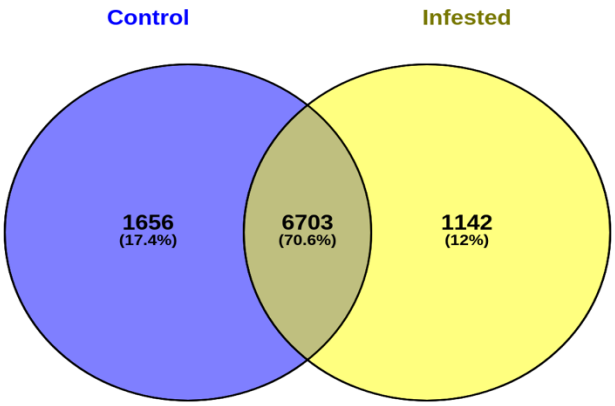

Fig. 4.13 A venn diagram showing number and proportion of lncRNAs expressed in the healthy/control and TMB-infested samples

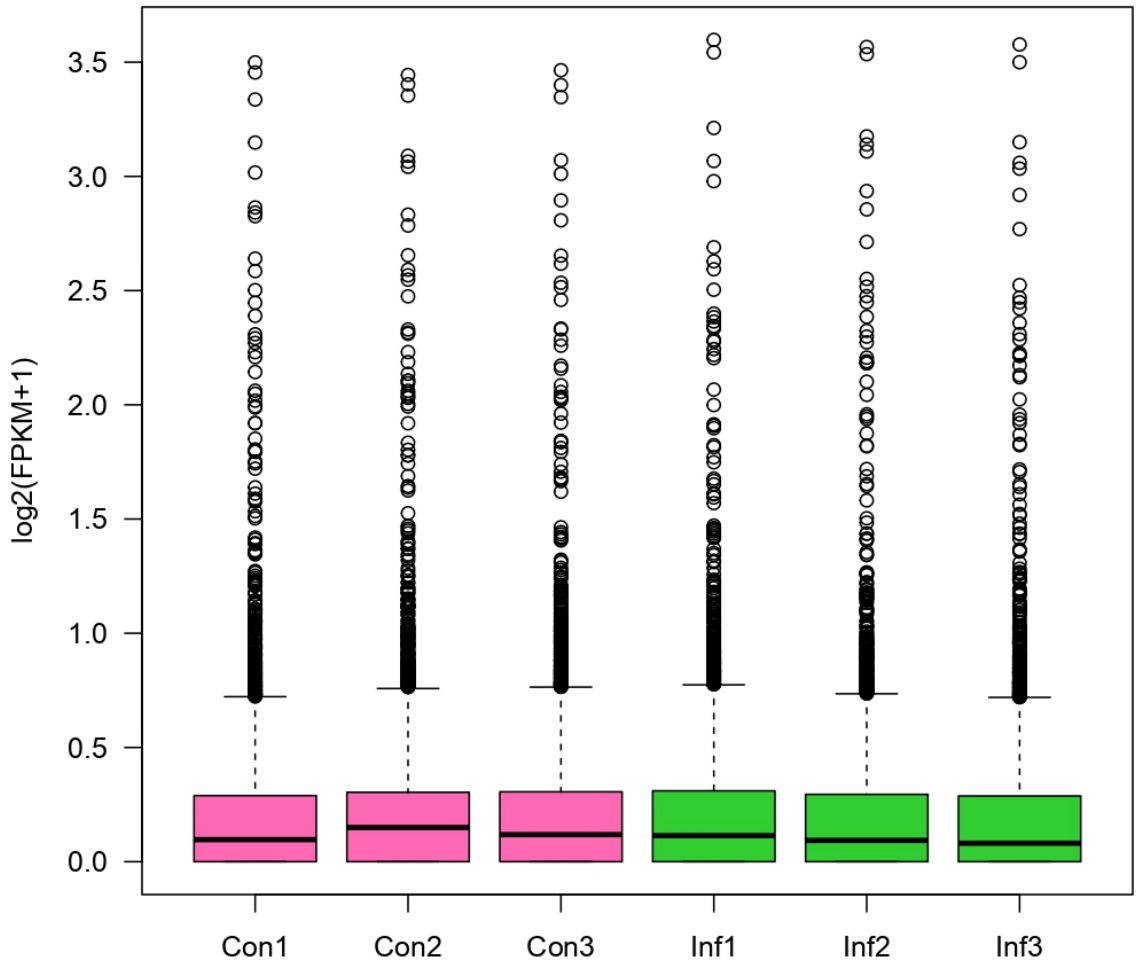

Fig. 4.14 Boxplot showing log2 values of FPKM+1 of lncRNAs in the healthy/control and TMB-infested samples

4.3.4 Differential expression of lncRNAs

To analyse the lncRNAs that were differentially abundant during healthy v/s infested condition, filtering out of lowly expressed lncRNAs was carried out and DE analysis was performed. It was revealed that 80 lncRNAs got differentially expressed in this study, out of which, expression of 46 DELs got down-regulated and 34 DELs got up-regulated in expression in the infested tissues.

Table. 4.2 List of DELs with their log2 fold change and p-values

lncRNA ids	log2FoldChange	padj (adjusted p-value)
TCONS_00116642	1.629913187	4.98E-32
TCONS_00102742	-3.04336472	9.04E-28
TCONS_00072135	-1.272696609	1.44E-17
TCONS_00123076	-5.233109775	1.44E-17
TCONS_00087320	-1.217454742	9.85E-16
TCONS_00078068	-1.354038746	1.28E-15
TCONS_00152106	-3.735200452	2.09E-13
TCONS_00076726	-3.08965386	6.08E-12
TCONS_00061691	2.634421841	9.74E-12
TCONS_00099260	-2.917861313	1.66E-11
TCONS_00040585	3.137312716	1.85E-11
TCONS_00025347	1.685679763	2.34E-11
TCONS_00024234	1.653065071	1.13E-10
TCONS_00028490	-2.154754878	1.94E-09
TCONS_00021732	1.481910798	4.38E-09
TCONS_00125414	-3.019906926	0.000000011
TCONS_00131931	2.898828059	2.26E-08
TCONS_00068537	1.710313098	2.94E-08
TCONS_00106979	-1.080193716	0.00000355
TCONS_00132530	-2.095719912	0.00000487
TCONS_00124553	-1.410040435	0.00000886
TCONS_00033045	-2.490444256	0.000207982
TCONS_00001085	1.328858679	0.000310822
TCONS_00149807	-1.939998024	0.000374853
TCONS_00032903	-1.723461579	0.000419851
TCONS_00125996	-1.260226525	0.000444479
TCONS_00057770	-1.457113911	0.000469516
TCONS_00083012	-1.804519284	0.000553373
TCONS_00115467	-1.428792536	0.000676592
TCONS_00096802	-1.448779234	0.00107357
TCONS_00104371	-2.37352162	0.00107357
TCONS_00015431	2.022460866	0.001078514
TCONS_00088006	1.415406426	0.00161464
TCONS_00096174	1.345072461	0.001729568
TCONS_00087056	2.653741968	0.001812695
TCONS_00030552	-1.298566434	0.002027731
TCONS_00030553	-1.293919388	0.00221069
TCONS_00038332	-2.188624516	0.002697755
TCONS_00017587	1.473745208	0.003767827
TCONS_00034064	1.555042651	0.00427081
TCONS_00032354	1.863903392	0.004689968
TCONS_00048159	-2.521670151	0.005162279
TCONS_00128571	-1.185455614	0.005375332

TCONS_00138715	1.590828065	0.007942299
TCONS_00083139	-2.344465683	0.009153549
TCONS_00038960	-1.038225519	0.00925177
TCONS_00126492	2.245784682	0.010059249
TCONS_00054633	2.723249984	0.011097888
TCONS_00147455	-1.625458509	0.012741807
TCONS_00143159	-1.800273796	0.012970215
TCONS_00073904	2.542205198	0.013820436
TCONS_00090137	1.484986476	0.017092866
TCONS_00114397	-1.652541158	0.017092866
TCONS_00083891	2.059948119	0.01807411
TCONS_00053665	-2.129413483	0.01807411
TCONS_00069554	-2.892179847	0.01807411
TCONS_00037756	-1.64049422	0.018164307
TCONS_00118970	1.11197076	0.020843541
TCONS_00062765	-1.86932069	0.020843541
TCONS_00063108	-1.376047338	0.021070118
TCONS_00070825	2.012492113	0.022920458
TCONS_00088007	1.554636651	0.023443674
TCONS_00108694	-2.830096319	0.024484914
TCONS_00027659	1.413824045	0.024574258
TCONS_00096953	1.005862266	0.024574258
TCONS_00096952	1.005862266	0.024574258
TCONS_00022462	-1.204577054	0.025985081
TCONS_00115148	2.561032362	0.026953448
TCONS_00129063	-1.309620635	0.026953448
TCONS_00041416	-1.56653296	0.026953448
TCONS_00038780	-2.199729209	0.027379295
TCONS_00054408	2.177851665	0.029646844
TCONS_00023432	2.293501192	0.033196624
TCONS_00039217	-1.149251467	0.033196624
TCONS_00060498	-1.221473001	0.033196624
TCONS_00152746	-1.244607982	0.033196624
TCONS_00025819	1.234634355	0.033591812
TCONS_00077127	-1.828108717	0.036260749
TCONS_00059256	2.250874959	0.039076601
TCONS_00024800	1.390618204	0.039076601

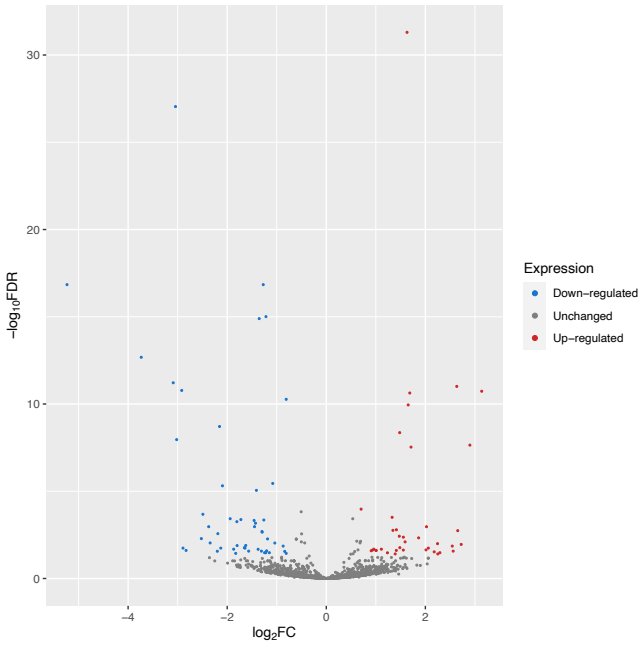

Fig. 4.15 Volcano plot showing the differential expression of lncRNAs in control v/s TMB-infested samples

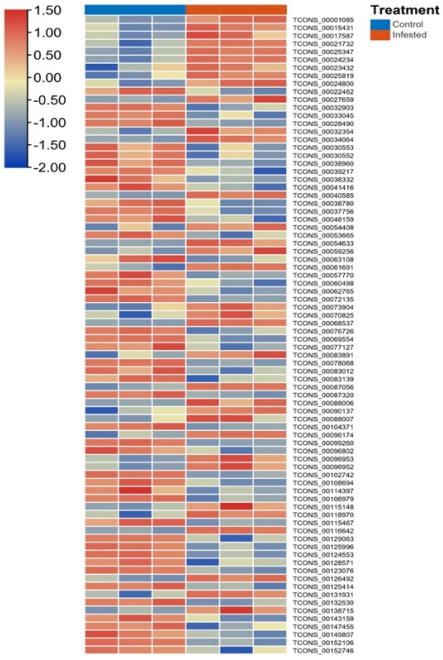

Fig. 4.16 Heatmap showing the differential expression pattern of lncRNAs in the six RNA-seq libraries. Blue colour represents low expression and red colour depicts high expression.

4.3.5 Identification of lncRNA-target genes

LncRNAs are reported to act on protein-coding genes through *cis* and *trans*-regulation. To find out potential protein-coding genes that might be regulated by lncRNAs through *cis*-acting mode, we screened for genes residing 10 kb upstream or downstream of identified lncRNAs. It was found that 2106 lncRNAs identified in this study were located in close proximity with 1916 protein-coding genes and these were identified as *cis*-targets of lncRNAs. The potential *trans*-acting effects of lncRNAs was determined for the genes by testing the RNA-RNA hybrid forming ability of lncRNA-mRNA pairs and co-expression analysis between DEL-DEG pairs applying stringent criteria for hybridization energy threshold and PCC respectively. A total of 787 genes were found to be *trans*-targets of lncRNAs by RNA-RNA hybrid forming potential of lncRNAs. The PCC for normalized expression values of DEL-DEG pairs was determined and pairs that did not meet the required criteria were discarded. In total, 76,442 positive and 49,553 negative associations were predicted for 80 DELs and 3509 DEGs. Summarizing the results we identified 5804 genes as potential lncRNA-targets.

Table. 4.3 Results of lncRNA-*cis* target hybrid formation analysis using RIBlast algorithm

Query name	Query Length	Target name	Target Length	Accessibility Energy	Hybridization Energy	Interaction Energy
TCONS_00003433	239	CSS0030542.1	1575	13.9607	-44.88	-30.9193
TCONS_00010009	222	CSS0004587.1	783	18.7477	-34.35	-15.6023
TCONS_00010009	222	CSS0032635.1	642	19.57	-40.94	-21.37
TCONS_00010009	222	CSS0018280.1	1359	16.0717	-42.58	-26.5083
TCONS_00010009	222	CSS0041917.1	687	18.9569	-40.71	-21.7531
TCONS_00010009	222	CSS0009579.1	681	17.1214	-38.66	-21.5386
TCONS_00010009	222	CSS0002303.1	2016	17.9971	-39.08	-21.0829

TCONS_00010009	222	CSS0035558.1	2481	15.795	-34.7	-18.905
TCONS_00016834	408	CSS0038642.1	2997	15.06	-55.21	-40.15
TCONS_00018213	658	CSS0033733.1	870	55.6281	-200.31	-144.682
TCONS_00033171	227	CSS0008052.1	1500	6.91269	-34.01	-27.0973
TCONS_00033171	227	CSS0018018.1	783	8.83517	-36.02	-27.1848
TCONS_00033171	227	CSS0018018.1	783	9.40424	-34.93	-25.5258
TCONS_00033171	227	CSS0037843.1	2076	3.48502	-33.21	-29.725
TCONS_00033171	227	CSS0009305.1	3294	7.54897	-34.85	-27.301
TCONS_00033171	227	CSS0002932.1	609	11.1142	-37.74	-26.6258
TCONS_00057665	641	CSS0032713.1	1731	13.8173	-36.48	-22.6627
TCONS_00057665	641	CSS0020268.1	3150	12.7416	-31.02	-18.2784
TCONS_00057665	641	CSS0005639.1	981	10.5824	-54.31	-43.7276
TCONS_00057665	641	CSS0041371.1	3810	16.2892	-34.7	-18.4108
TCONS_00057665	641	CSS0008429.1	1401	19.4689	-38.68	-19.2111
TCONS_00057665	641	CSS0038642.1	2997	11.8746	-35.95	-24.0754
TCONS_00057665	641	CSS0048765.1	840	13.2746	-40.79	-27.5154
TCONS_00057665	641	CSS0036298.1	627	13.3758	-31.7	-18.3242
TCONS_00057665	641	CSS0007810.1	1794	15.8229	-37.49	-21.6671
TCONS_00057665	641	CSS0037673.1	1095	11.4089	-33.15	-21.7411
TCONS_00057665	641	CSS0037673.1	1095	12.5475	-32.79	-20.2425
TCONS_00087135	358	CSS0008052.1	1500	6.20285	-32.57	-26.3671
TCONS_00087135	358	CSS0037843.1	2076	3.77097	-34.51	-30.739

4.3.6 Functional annotation and enrichment analysis of lncRNAs

The functional annotation and enrichment analysis of lncRNA-targets revealed that these genes were enriched in 378 GO terms including 310 under biological process, 30 under cellular component and 38 under molecular function. The top 30 terms are being shown in Fig. 4.17. It is interesting to note that expression of lncRNA-targets were suppressed in GO terms related to cell cycle, nuclear division, organelle fission. Whereas a significant set of genes were upregulated in GO terms associated with cellular response to phosphate

starvation, transferase, oxidoreductase and dioxygenase activity, response to chemical/oxygen-containing compound, metal-ion binding etc. (Fig. 4.18).

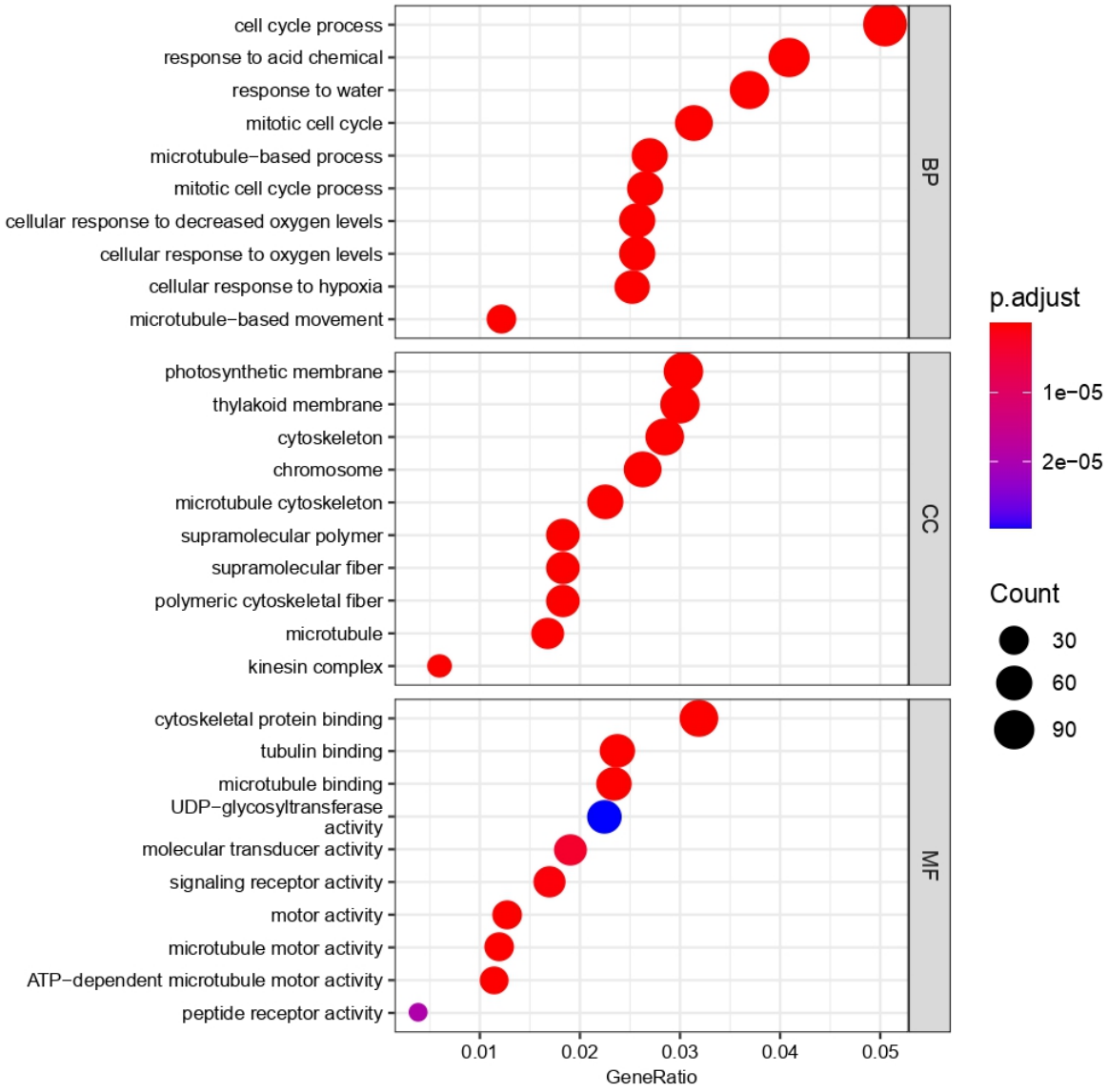

Fig. 4.17 GO enrichment of lncRNA-target genes. BP; Biological processes, CC; Cellular component, MF; Molecular function. The size of the bubble represents number of lncRNA-target genes assigned to the particular GO term and the color of the bubble represents adjusted p-value (q value).

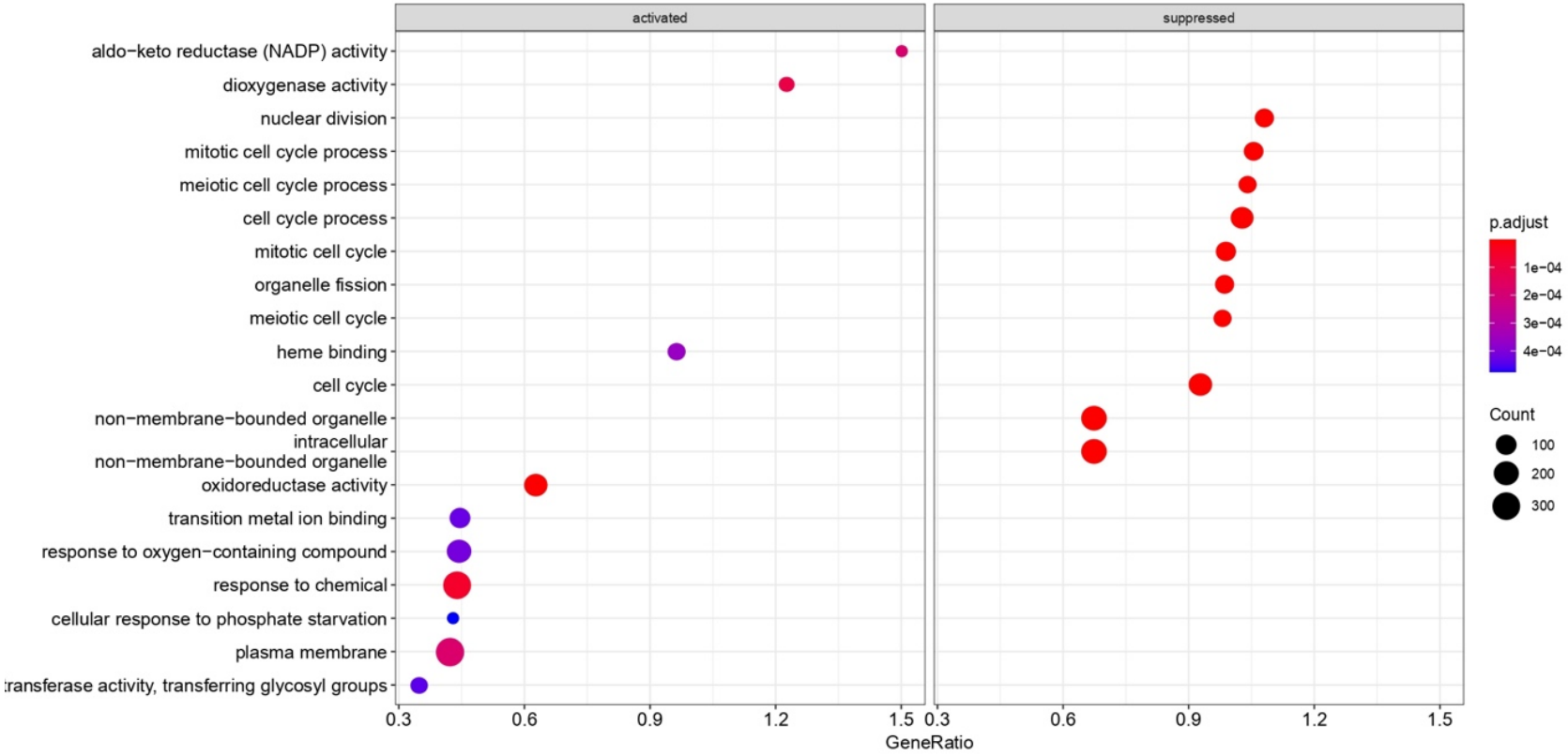

Fig. 4.18 Gene set enrichment analysis based on GO enrichment of lncRNA-target genes. The left halve represents terms upregulated in response to TMB and the right halve represents terms downregulated in response to TMB. The size of the bubble represents number of lncRNA-target genes assigned to the particular GO term and the color of the bubble represents adjusted p-value (q value).

Additionally, GSEA for KEGG pathways has shown that lncRNA-target genes were enriched in 20 KEGG pathways, out of which, pathways like biosynthesis of N-glycans, endocytosis, amino sugar and nucleotide sugar metabolism were suppressed. In contrast, pathways related to photosynthesis, biosynthesis of secondary metabolites, terpenoids biosynthesis, metabolic pathways of certain amino acids like beta-alanine tryptophan, cysteine, methionine, tyrosine got activated (Fig 4.19).

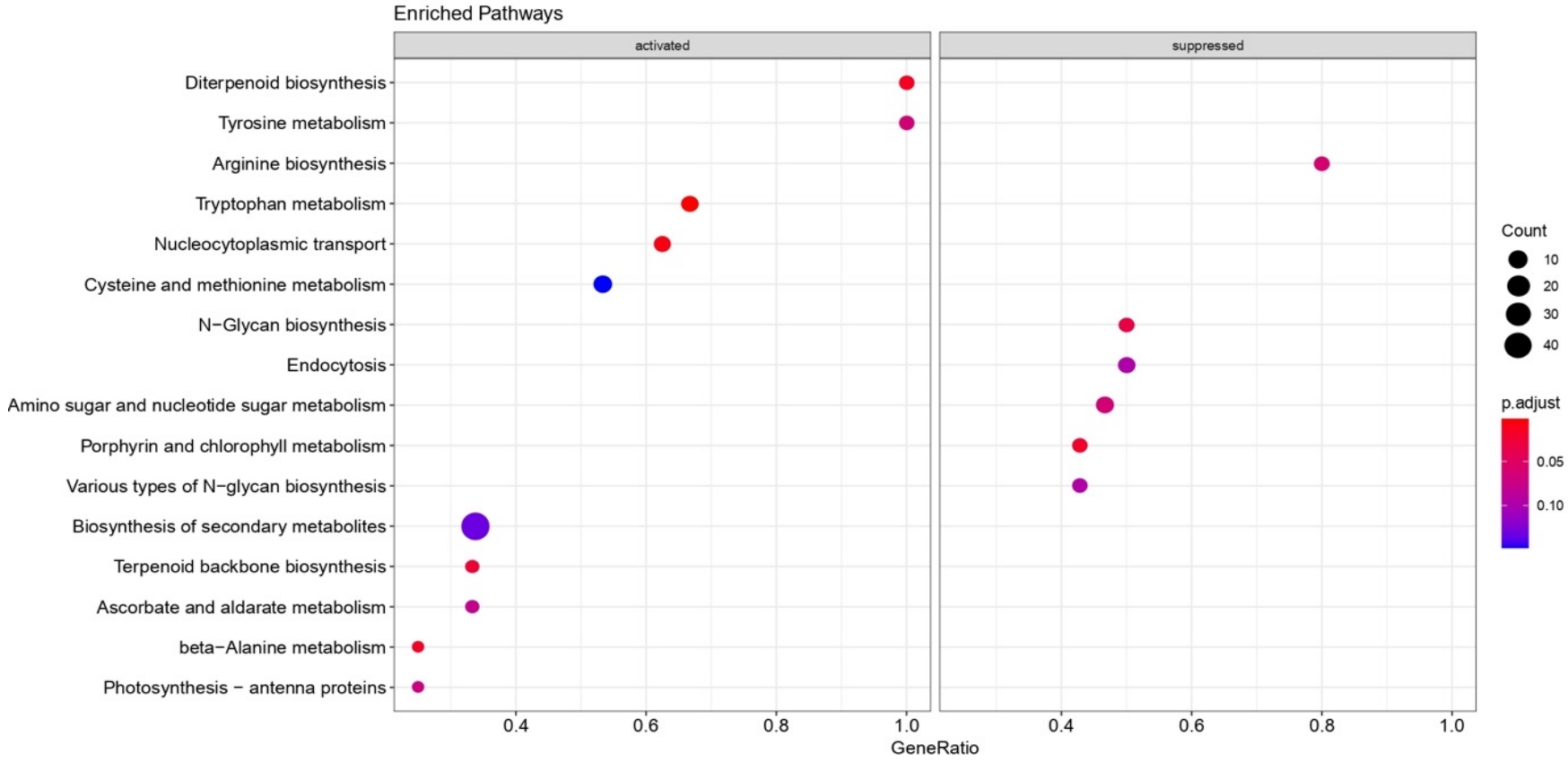

Fig. 4.19 Gene set enrichment analysis based on KEGG pathway enrichment of lncRNA-target genes. The left halve represents pathways upregulated in response to TMB and the right halve represents pathways downregulated in response to TMB. The size of the bubble represents number of lncRNA-target genes assigned to the particular KEGG pathway and the color of the bubble represents adjusted p-value (q value).

To understand the possible functions of identified lncRNAs, further pathway mapping for the lncRNA-target genes was performed using the BlastKOALA web version (Kanehisa *et al*. 2016). Results showed that the lncRNA-target genes belonged to certain important pathways. Some of them include terpenoid biosynthesis, flavonoid biosynthesis, zeatin biosynthesis, plant hormone signal transduction, MAPK signalling pathway, linoleic-acid metabolism, brassinosteroid biosynthesis. LncRNA-target genes belonging to the above-mentioned pathways were also screened for their expression patterns during TMB-infested and non-infested conditions. The expression heatmaps for lncRNA-target genes associated with these pathways is represented in Fig. 4.20.

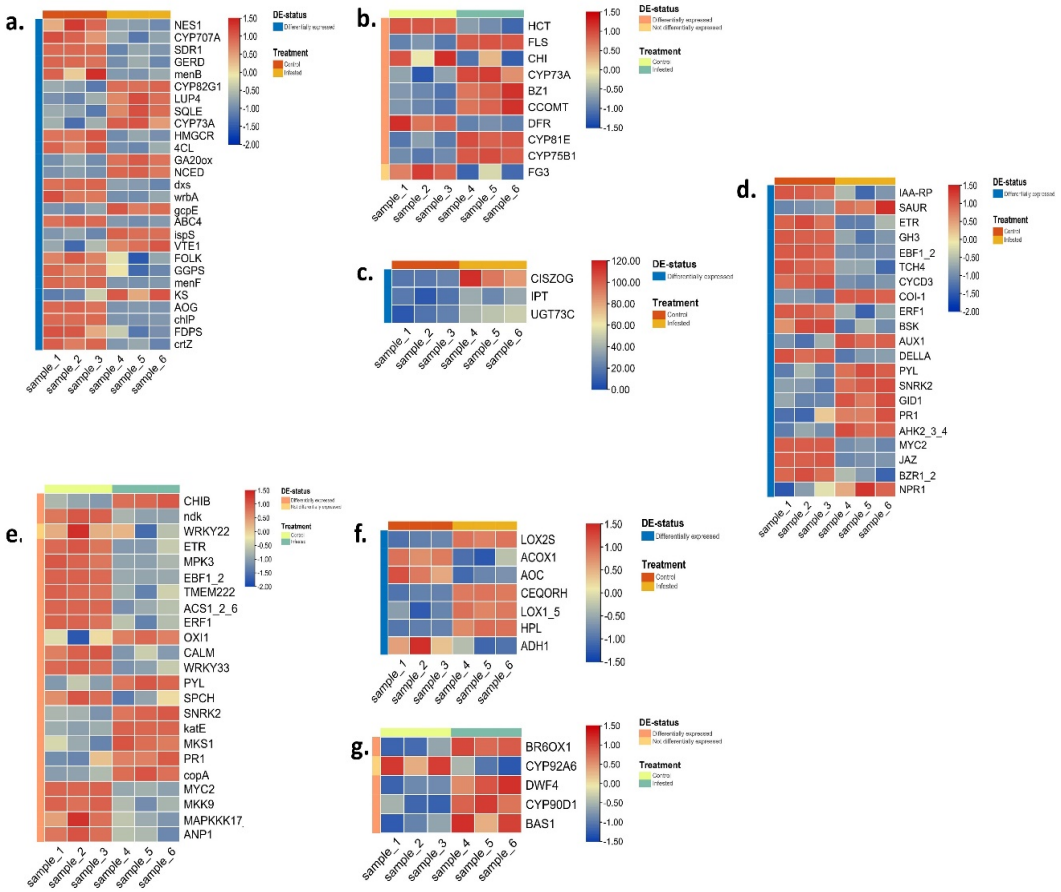

Fig. 4.20 Heatmaps showing expression patterns of lncRNA-target genes in different biological pathways (a) Terpenoids biosynthesis (b) Flavonoids biosynthesis (c) Zeatin biosynthesis (d) Plant hormone signal transduction (e) MAPK signaling pathway (f) Linoleic-acid metabolism (g) Brassinosteroids biosynthesis

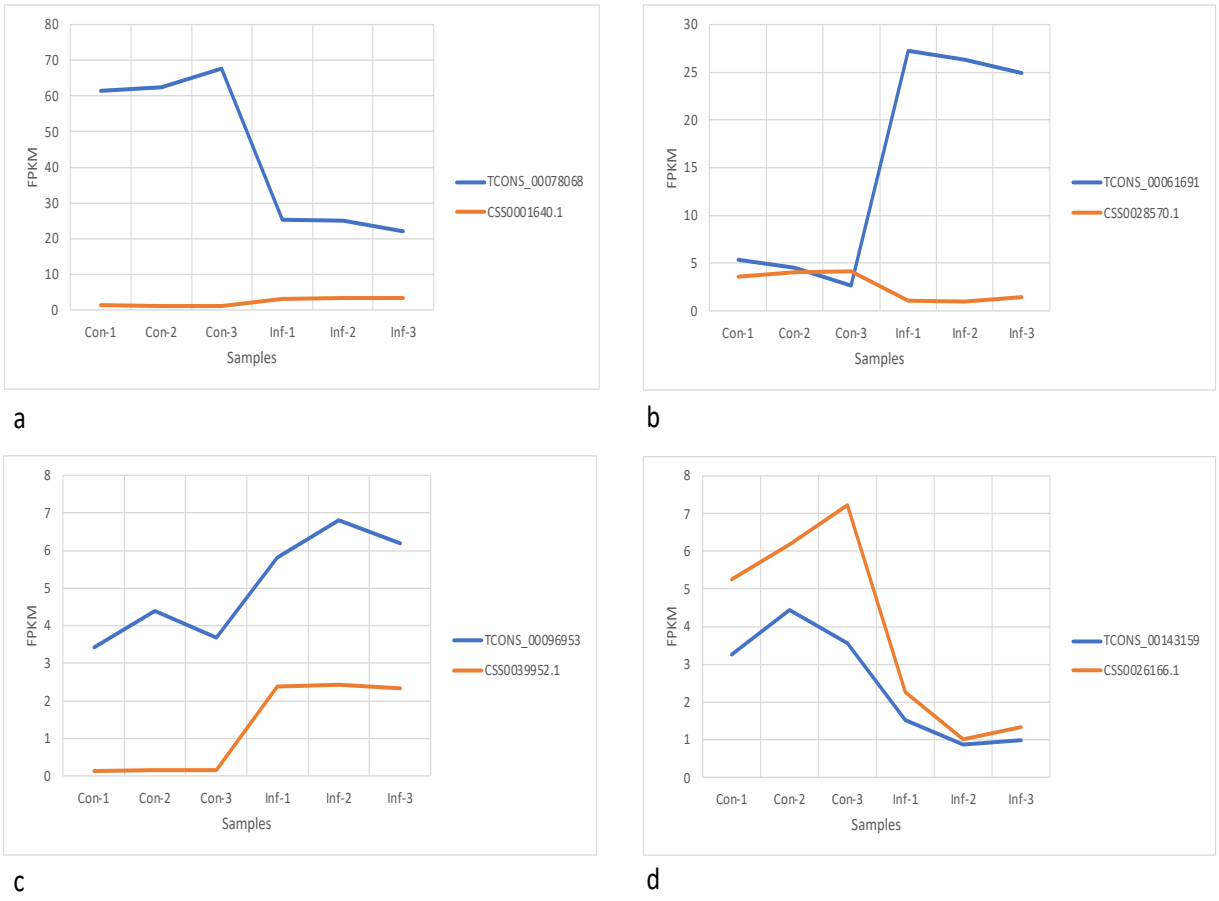

Fig. 4.21 Graphs showing positive/negative expression correlation between lncRNA and lncRNA-target genes. Blue line signifies FPKM values (x-axis) of lncRNAs and red line signifies FPKM values (x-axis) of lncRNA-target genes. Figures a and b denote negative correlation between lncRNA-mRNA pairs, figures c and d denote positive correlation between the pairs.

4.3.7 Quantitative real-time PCR of selected DELs

The qRT-PCR result has shown the differential up/down regulation of DELs selected for this analysis. The qRT-PCR analysis reveals that the expression of selected lncRNAs was found to be more or less consistent with the results of RNA-seq data.

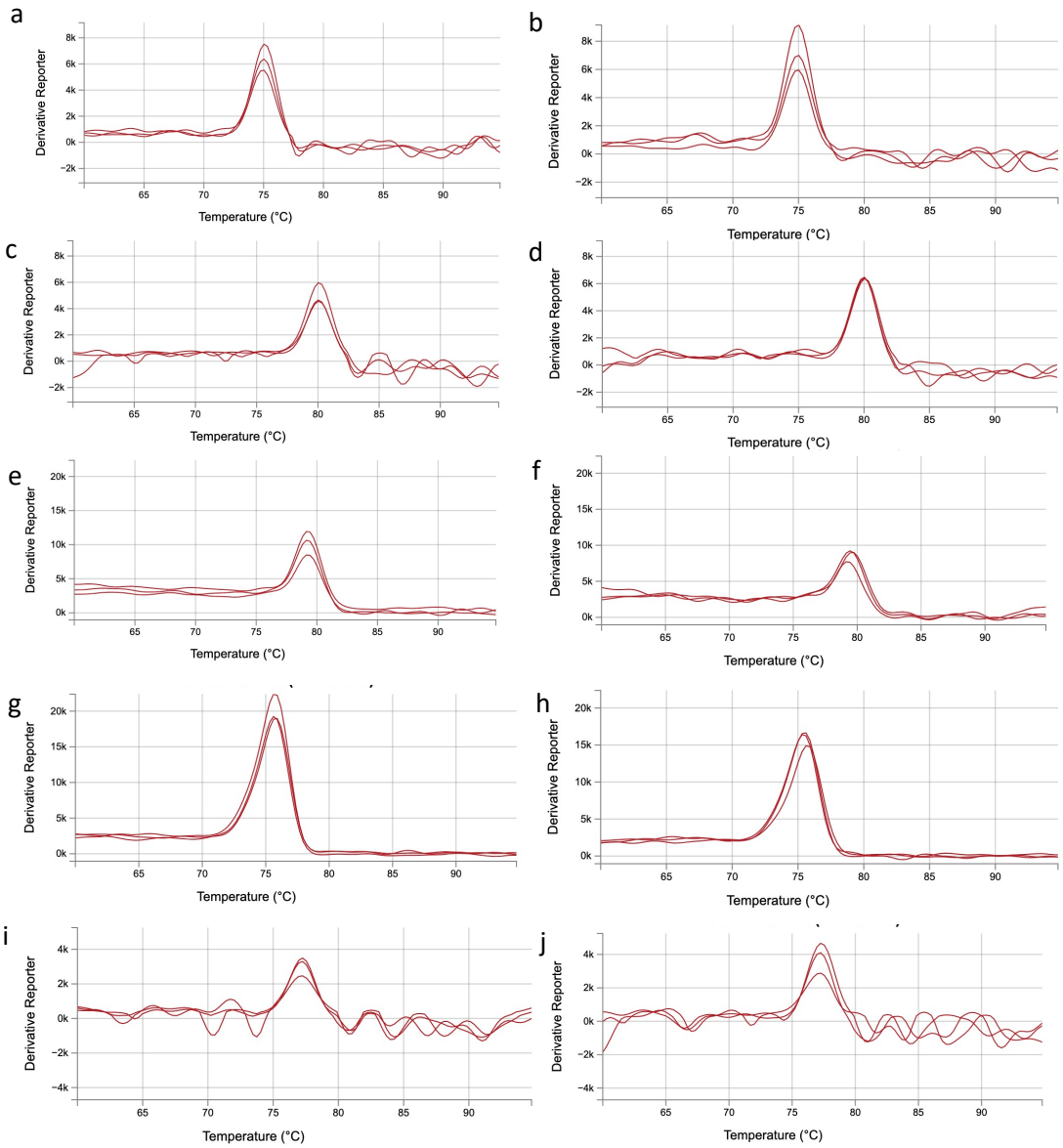

Fig. 4.22 Melt curve plots of DELs TCONS_00040585 (a and b), TCONS_00083891 (c and d), TCONS_00096174 (e and f), TCONS_00032903 (g and h) and TCONS_00099260 (i and j) in control and TMB-infested samples

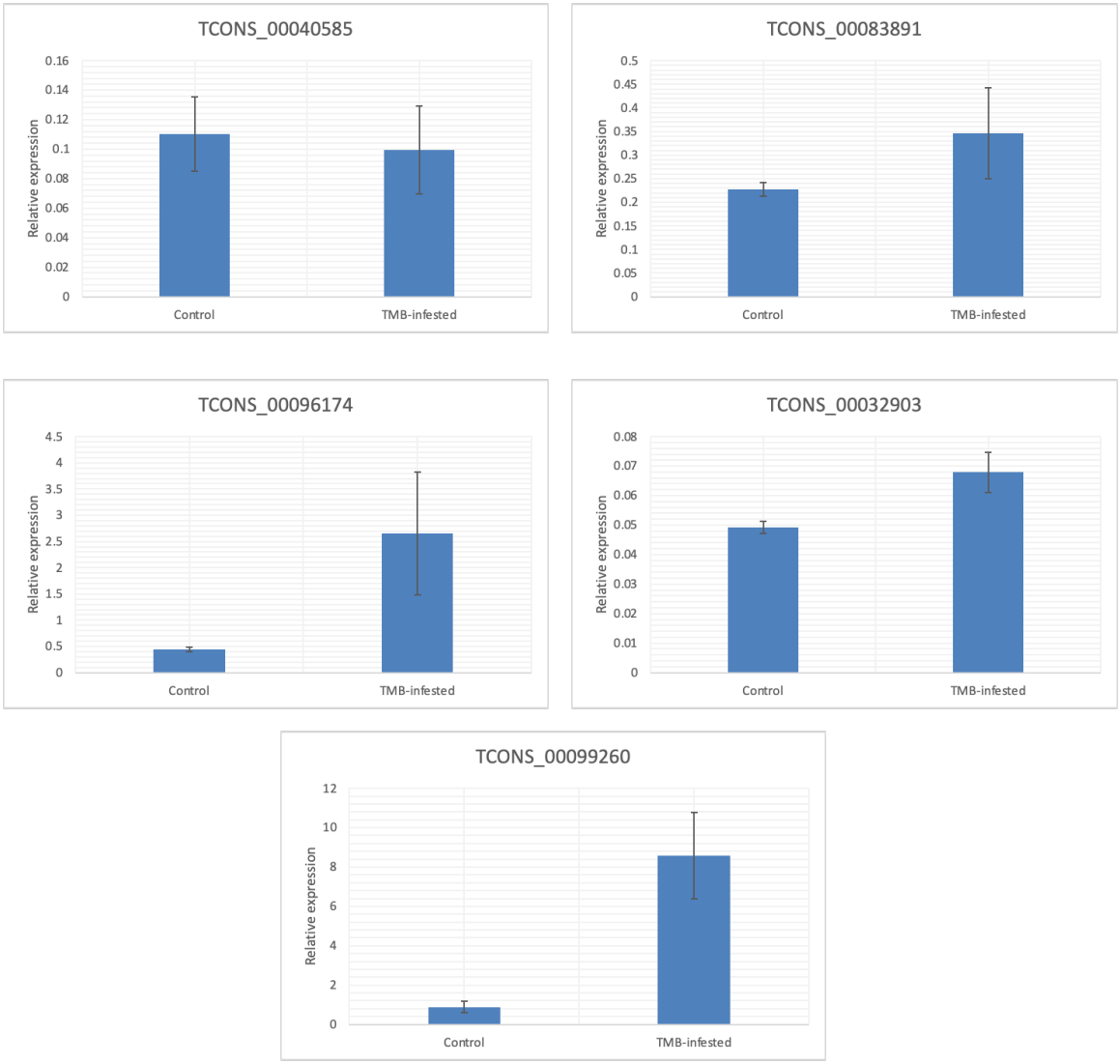

Fig. 4.23 Bar diagrams showing result of qRT-PCR analysis of 5 DELs in control v/s TMB-infested samples. Values in the y-axis determine the relative expression of DELs normalized to UBC1 gene. Error bars indicate ±SEM of relative expression of triplicates.

4.4 Genes

4.4.1 Expression of genes

StringTie software was used to estimate the FPKM values for genes and 36644 genes were found to be expressed in at least one of the RNA-seq libraries of this study. The FPKM values of the genes in the libraries has been visualized in Fig. 4.24.

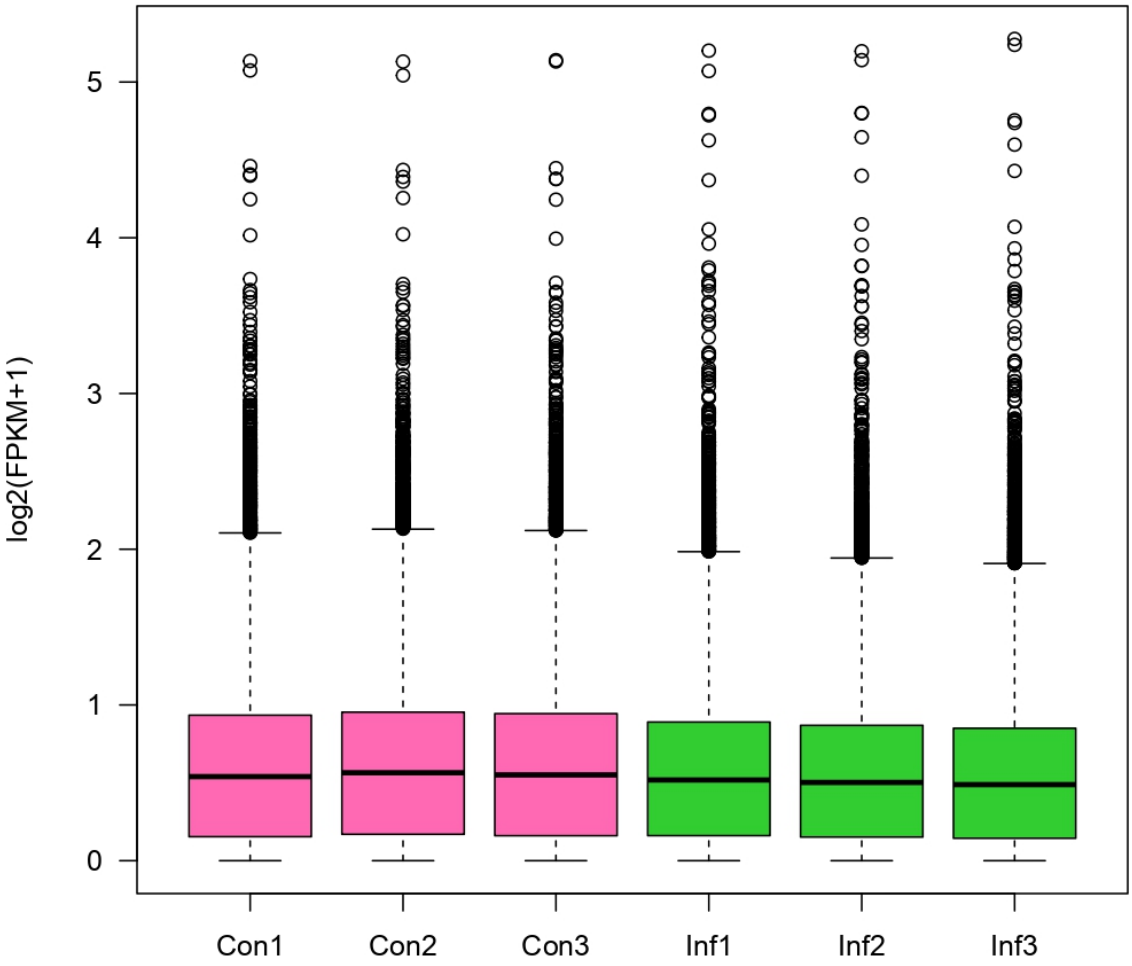

Fig. 4.24 Boxplot showing log2 values of FPKM+1 of genes in the healthy/control and TMB-infested samples

Expression of 1599 genes were limited to only the infested tissues whereas 2375 genes were expressed only in the healthy/uninfested leaves.

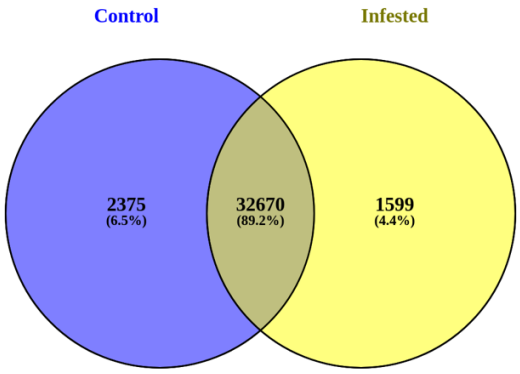

Fig. 4.25 A venn diagram showing number and proportion of genes expressed in the healthy/control and TMB-infested samples

4.4.2 Differential expression of genes

DE analysis revealed that 3665 genes were differentially expressed during healthy v/s infested condition, of which 1767 genes showed increase in expression and 1898 showed decreased expression in the TMB infested *C. sinensis* tissues. The apparent expression variations in DEGs are visualized using volcano plots and heatmaps (Fig. 4.26).

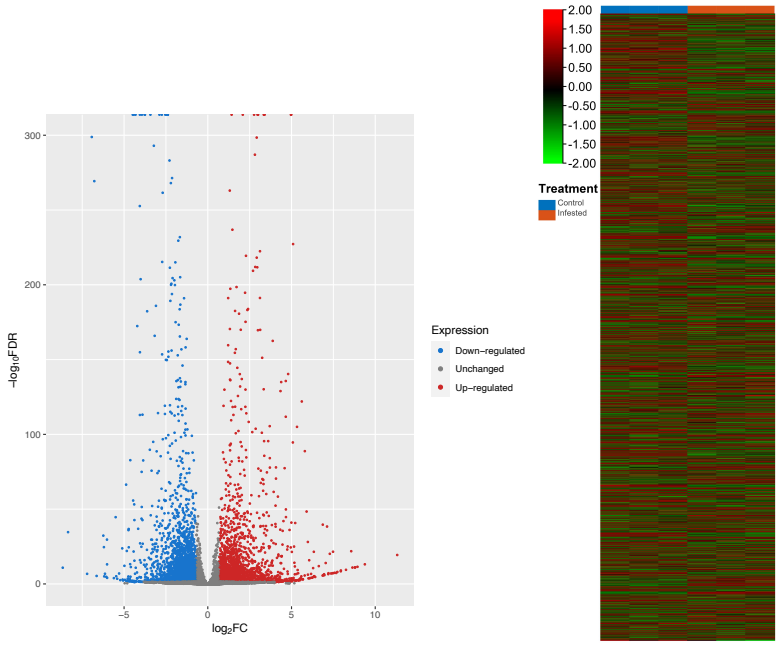

Fig. 4.26 Volcano plot and expression heatmap depicting DEGs

4.4.3 Functional annotation and enrichment analysis of DEGs

The GSEA of differentially expressed genes elucidated that a significant set of genes were associated with 771 GO terms (481 under biological process, 103 under cellular compartment and 187 under molecular function) and the expression of the gene sets were either suppressed or activated in the GO terms. Gene sets of DEGs were activated in GO terms like “secondary metabolic process”, “response to external biotic stimulus”, “response to other organism”, “oxidoreductase activity”, “dioxygenase activity” etc., which revealed that the DEGs are involved in response of the tea plant to biotic stress or foreign biotic stimuli like insect elicitors. Adding to that, set of genes in GO terms like “mitotic cell cycle process”, “nuclear division”, “microtubule motor activity and binding”, “organelle fission” etc. were found to be suppressed during the infested condition (Fig. 4.27).

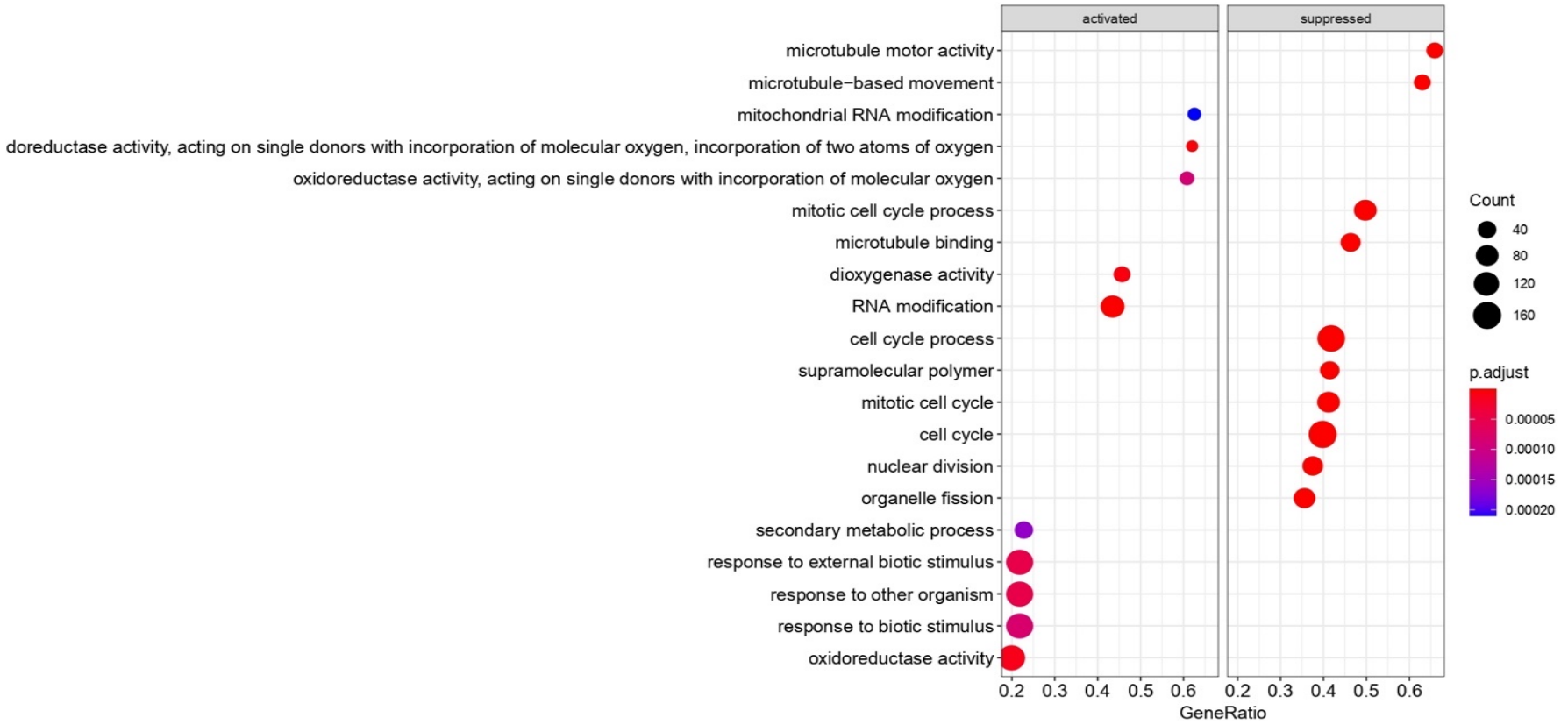

Fig. 4.27 Gene set enrichment analysis based on GO enrichment of DEGs. The left halve represents terms upregulated in response to TMB and the right halve represents terms downregulated in response to TMB. The size of the bubble represents number of DEGs assigned to the particular GO term and the color of the bubble represents adjusted p-value (q value).

The DEGs were found to be enriched in 26 significant KEGG pathways. In response to TMB infestation, significant set of genes were activated in 17 KEGG pathways including those for terpenoids metabolism, cell signalling pathways (MAPK), amino acid metabolism like tryptophan and cyanoamino acid (Fig. 4.28). Terpenoids possess insect/pathogen deterrent properties and have significant role in plant-insect interaction such as priming defense responses in neighbouring plants (Sharma *et al*. 2017). Upregulation of terpenoid synthesizing genes in our study signifies the involvement of terpenoids in tea plant's defense against the feeding insect. MAPKs play critical role in activation of herbivore induced defense responses in plants by accumulation of plant defense metabolites against insects and modulate herbivory induced phytohormonal dynamics of SA, JA and ET. Two MAPKs viz. salicylic-acid induced protein kinase (SIPK) and wound induced protein kinase (WIPK) get rapidly induced in response to insect OS and play roles in PAMPs (Pathogen associated molecular patterns) triggered immunity or PTI. Activation of MAPKs in response to wounding and insect herbivory has been observed in many studies (Seo *et al*. 1995; Wu *et al*. 2007; Kandoth *et al*. 2007; Sözen *et al*. 2020). Induction in expression of genes related to MAPK signalling pathway in this study is indicative of the involvement of MAPKs in tea plant's response to TMB. Tryptophan is associated with the production of phytohormone auxin and plant defensive compounds (Celenza, 2001), therefore upregulation of genes belonging to tryptophan metabolism pathway is self-explanatory. Additionally, genes for zeatin, betalain and alkaloids biosynthesis, all of which have well-known defensive functions, were also seen to get upregulated in this study. Concomitantly, 9 KEGG pathways got suppressed during TMB infestation on *C. sinensis*. This includes carotenoids and amino acids biosynthesis, base excision repair (BER),

amino and nucleotide sugar metabolism etc. Exposure to abiotic/biotic stresses leads to DNA damage and maintenance of genome integrity in eukaryotes is executed by DNA repair mechanisms like BER (Nisa *et al*. 2019). Literature suggests that microbial pathogens induce DNA double-strand breaks in host plant DNA (Song and Bent, 2014) and hence it can be speculated that suppression of BER mechanism in the tea plant is an indication of successful pathogenesis. Changes in carbohydrate (sugar) and nitrogen (amino acids) metabolism during insect stress can be either attributed to a means of plant defense response or to insect manipulation of host plant metabolism.

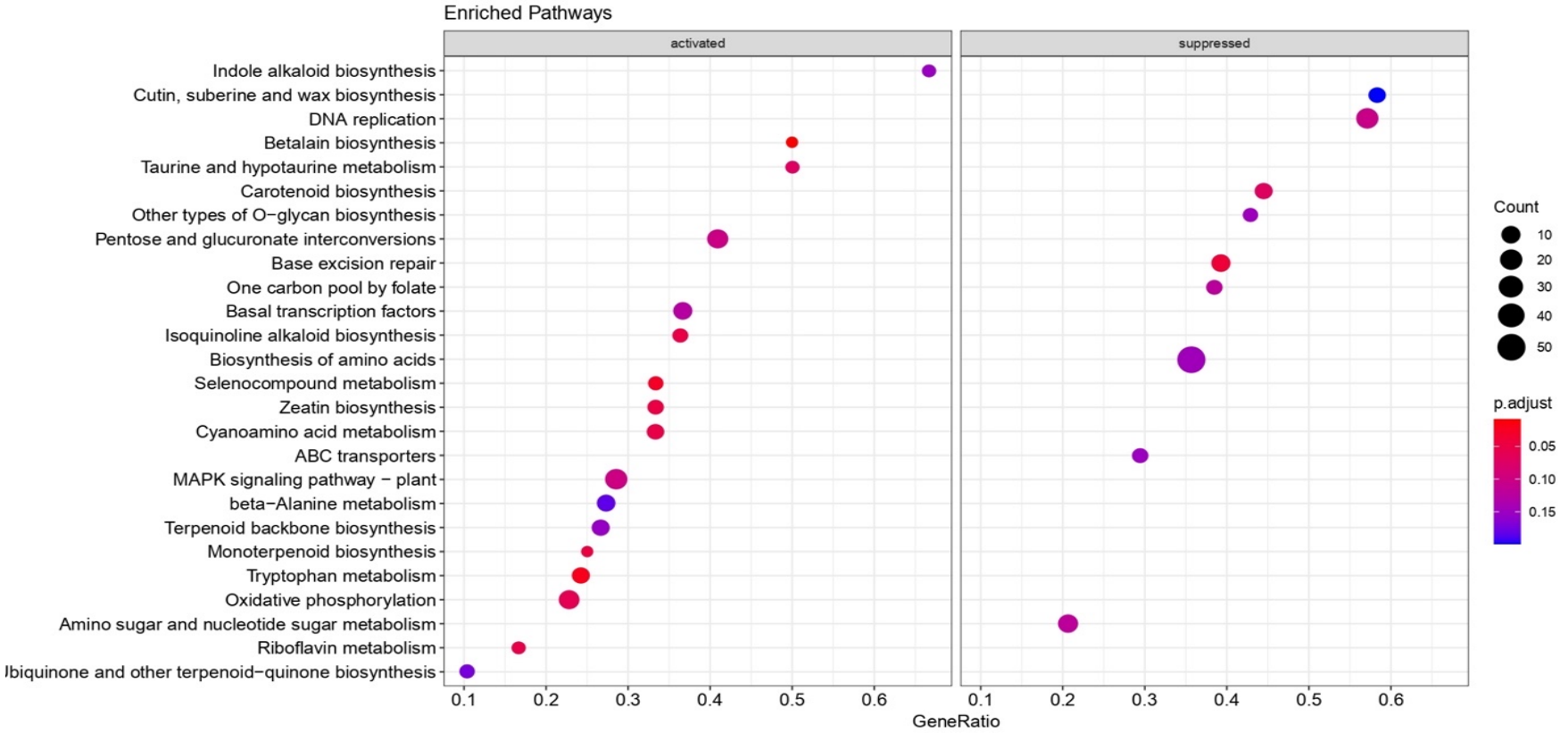

Fig. 4.28 Gene set enrichment analysis based on KEGG pathway enrichment of DEGs. The left halve represents pathways upregulated in response to TMB and the right halve represents pathways downregulated in response to TMB. The size of the bubble represents number of DEGs assigned to the particular KEGG pathway and the color of the bubble represents adjusted p-value (q value).

4.4.4 Quantitative real-time PCR of selected DEGs

The result of qRT-PCR has validated the differential expression pattern of the 6 selected DEGs. The qRT-PCR results of the selected DEGs was found to be more or less consistent with the RNA-seq data (Fig. 4.29 and 4.30).

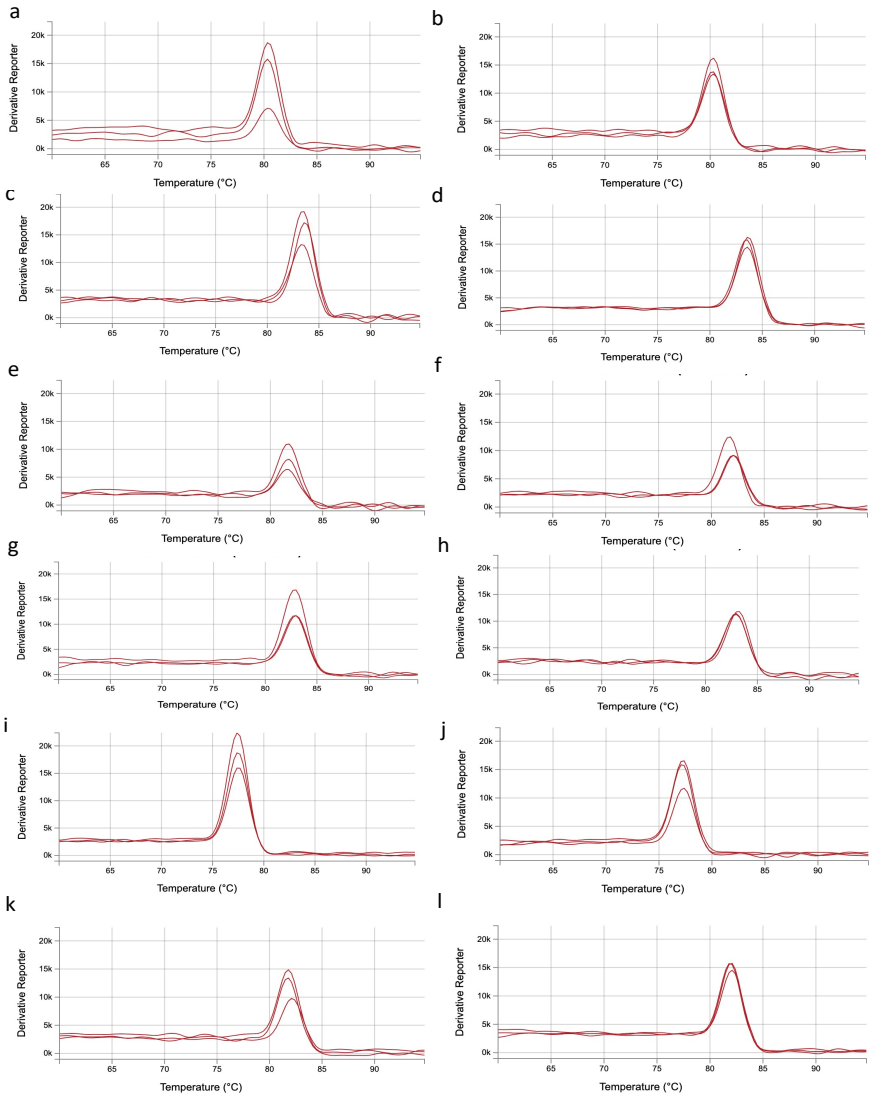

Fig. 4.29 Melt curve plots of DEGs CSS0024393.1 (a and b), CSS0006785.2 (c and d), CSS0016212.1 (e and f), CSS0018684.1 (g and h), CSS0023703.1 (i and j) and CSS0046901.1 (k and l) in control and TMB-infested samples

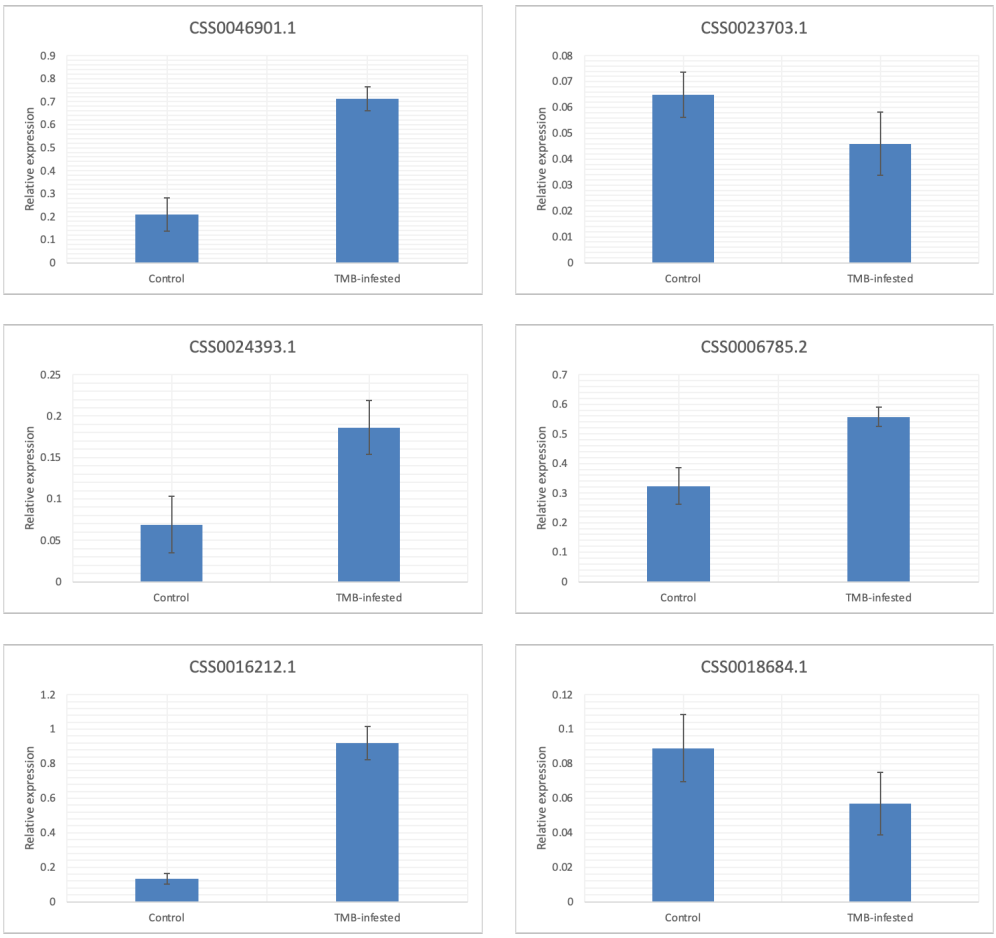

Fig. 4.30 Bar diagrams showing result of qRT-PCR analysis of 6 DEGs in control v/s TMB-infested samples. Values in the y-axis determine the relative expression of DEGs normalized to UBC1 gene. Error bars indicate ±SEM of relative expression of triplicates.

4.5 Comparison between lncRNAs and mRNAs identified in this study

The length distribution and exon numbers of lncRNAs were compared with those of mRNAs to further illustrate the features of candidate lncRNAs of *C. sinensis*. Most of the lncRNAs (62.14%) were found to be < 400 nucleotides in length and only a few of them (4.58%) were longer than 1000 bp. Whereas mRNAs with length > 1000 nucleotides accounted for 60.15% (Fig. 4.31a). The lncRNAs exhibited exon numbers in a range of

2-8 where 83.6% comprised of two exons and only 0.01% had eight exons. In contrast, mRNAs had exon numbers ranging from 1-77 and 16.01% mRNAs have ≥ 10 exons (Fig. 4.31b). These findings are consistent with previous reports (Wan *et al*. 2020; Zou *et al*. 2020; He *et al*. 2019; Tian *et al*. 2020) which support the fact that lncRNAs are shorter in length and contain less exon numbers as compared with the mRNAs. Comparison of expression levels of lncRNAs and mRNAs based on their FPKM values in the six libraries is being shown in Fig. 4.31c. The lncRNAs in this study showed lower FPKM values than genes and this is in accordance with previous studies (Tian *et al*. 2021; Zou *et al*. 2020).

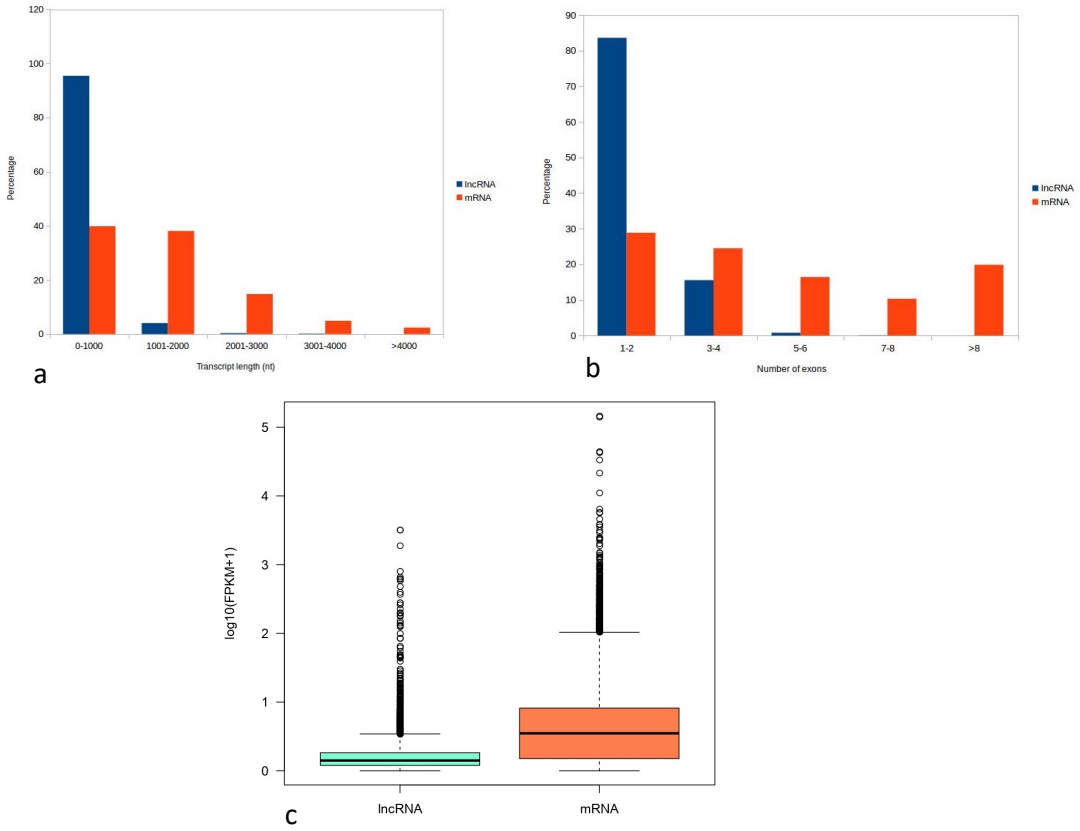

Fig. 4.31 (a) Bar diagram showing distribution of transcript length of both identified lncRNAs and expressed mRNAs (b) Comparison of exon numbers between identified lncRNAs and mRNAs (c) Boxplot showing distribution of FPKM values of lncRNAs and mRNAs

4.6 CircRNAs

4.6.1 Identification and characterization of circRNAs

We obtained an average of 39902058 number of clean reads in the control samples and 45566217 reads in the TMB-infested samples through the high-throughput sequencing. Based on the sequenced reads, the CIRI2 tool predicted 709 circRNAs in total from six RNA-seq libraries. Distribution pattern of circRNAs in the 15 chromosomes of *C. sinensis* genome showed that chromosome 1 contained the highest number of identified circRNAs (66).

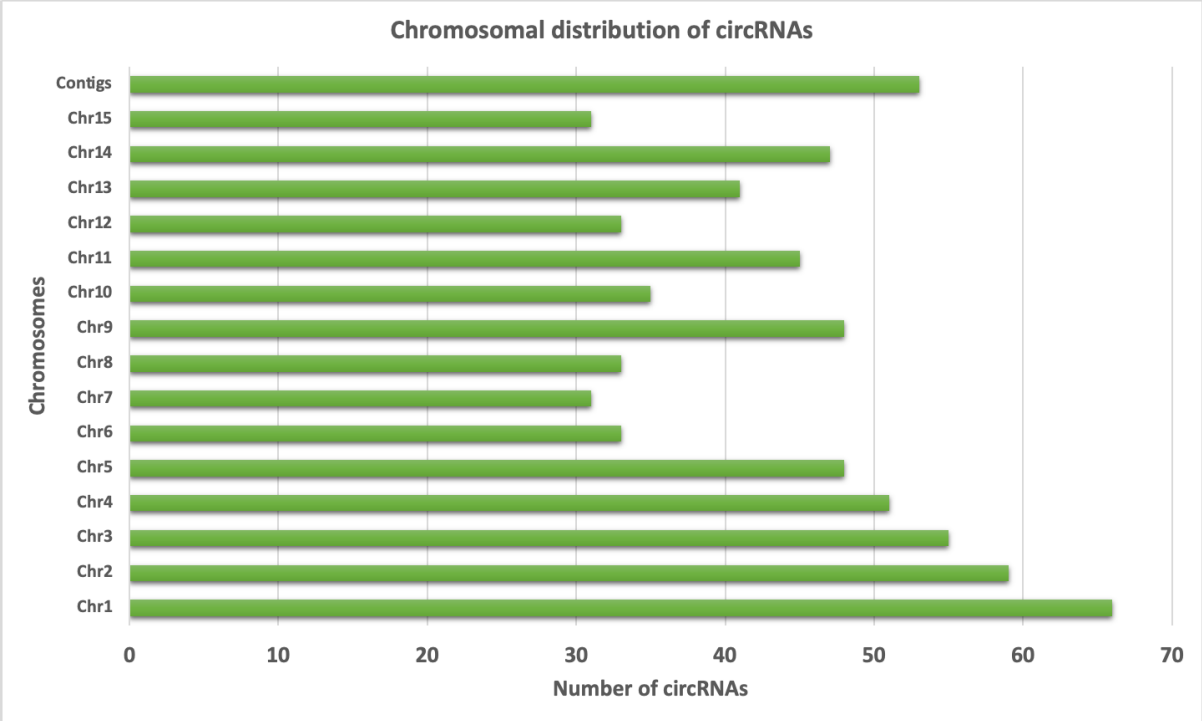

Fig. 4.32 Chromosomal distribution of identified circRNAs

They were classified according to their genomic positions and majority of them (62%) were derived from intergenic regions, followed by exonic (35%) and intronic circRNAs (3%) (Fig. 4.33a). The healthy and TMB infested tissues shared 30.3% of the circRNAs in common, while 209 (29.5%) circRNAs were expressed selectively in TMB infested

tea leaves (Fig. 4.33b). The length of the circRNAs ranged from 138-5000+ nucleotides and the proportion of circRNAs with lengths greater than 5000 bp is the highest (58.11%). The length distribution of circRNAs has been displayed in Fig. 4.33c. We also perfomed a BLASTn search to analyse whether the identified circRNAs are evolutionarily conserved among other plant species. About 60% (425 circRNAs) of the identified circRNAs showed homology with already known plant circRNAs deposited in the PlantcircBase. CircRNAs of this study showed homology with circRNAs of 12 plant species. The highest homology was recorded from previously reported circRNAs of *C. sinensis* found in PlantcircBase, followed by those of *Zea mays, Oryza sativa, Gossipium hirsutum, Populus trichocarpa, Solanum lycopersicum* (Fig. 4.33d).

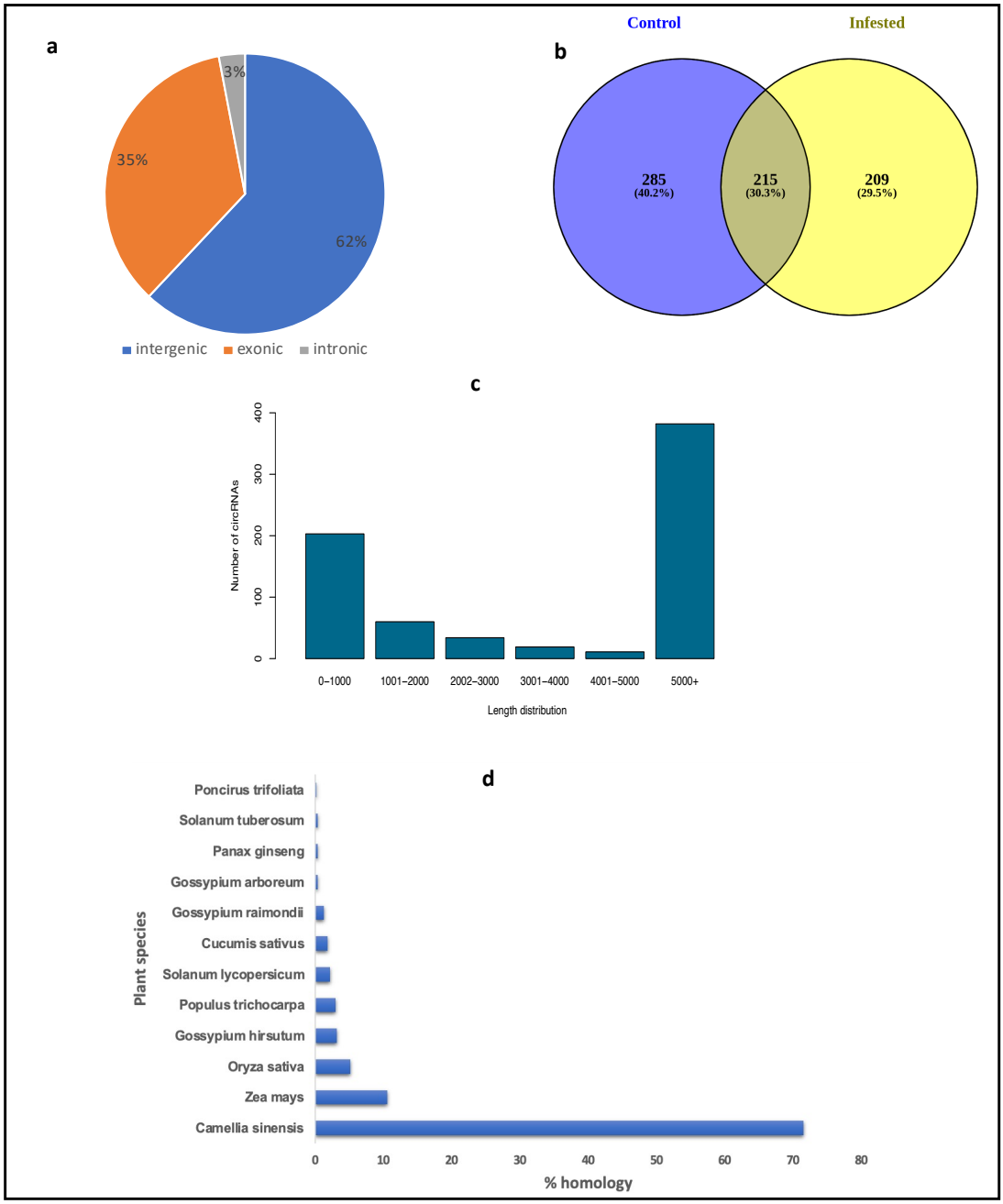

Fig. 4.33 Characterization of identified circRNAs in tea plant. (a) Pie chart showing classification of circRNAs based on their genomic positions (b) Venn diagram showing number of unique and common circRNAs identified in control and TMB-infested samples (c) Bar diagram showing length distribution of identified circRNAs (d) Percentage of circRNAs showing homology with already reported circRNAs of different plant species deposited in PlantcircBase

4.6.2 The differential expression pattern of identified circRNAs

The precise expression of circRNAs infers their probable involvements with specific biological functions. To check whether circRNAs were differentially abundant during control v/s treated condition, we compared the expression patterns of circRNAs in the healthy tea plants (control) v/s TMB-treated group of tea plants. We observed a distinct expression pattern of circRNAs in both the control and treatment group of plants. It was found that out of the 709 identified circRNAs, 34 circRNAs got differentially expressed during TMB treatment on tea plant. This includes 15 up-regulated and 19 down-regulated circRNAs which indicated their possible role in TMB stress on tea plant. Fig. 4.34a and 4.34b represent the differential expression visualization of DECs through heatmap and volcano plot respectively.

Table. 4.4 List of DECs with their log2 fold change and p-values

circRNA id	**Log2 fold change**	**Adjusted p-value (padj)**
Csi-circ4	2.053325	0
Csi-circ120	1.703429	1.85E-272
Csi-circ51	-2.1504	2.52E-235
Csi-circ694	1.393367	3.30E-232
Csi-circ385	-1.5555	1.41E-167
Csi-circ203	2.847199	1.56E-91
Csi-circ391	-1.99755	2.75E-67
Csi-circ245	-3.32441	2.46E-44
Csi-circ180	1.940574	2.52E-35
Csi-circ404	-1.90451	2.14E-31
Csi-circ282	-1.38954	1.58E-30
Csi-circ394	-1.35273	3.93E-29
Csi-circ593	-1.60034	8.38E-19
Csi-circ47	-2.03786	6.07E-17
Csi-circ321	-2.34697	7.15E-13
Csi-circ594	-1.07181	9.32E-12
Csi-circ598	1.064933	1.16E-11
Csi-circ680	3.940519	1.28E-11
Csi-circ330	-1.05856	2.27E-11
Csi-circ243	-3.06236	2.36E-10
Csi-circ150	1.866072	2.93E-10

Csi-circ87	1.126929	6.97E-09
Csi-circ186	-1.47149	3.98E-07
Csi-circ666	-1.59185	6.36E-06
Csi-circ428	-2.18795	1.39E-05
Csi-circ701	-1.80081	2.14E-05
Csi-circ130	-1.37495	2.20E-05
Csi-circ357	2.400324	5.50E-05
Csi-circ331	1.485547	0.000341
Csi-circ623	-1.01008	0.000769
Csi-circ389	1.088886	0.004986
Csi-circ219	1.382156	0.006061
Csi-circ453	2.004185	0.011813
Csi-circ458	1.45577	0.03905

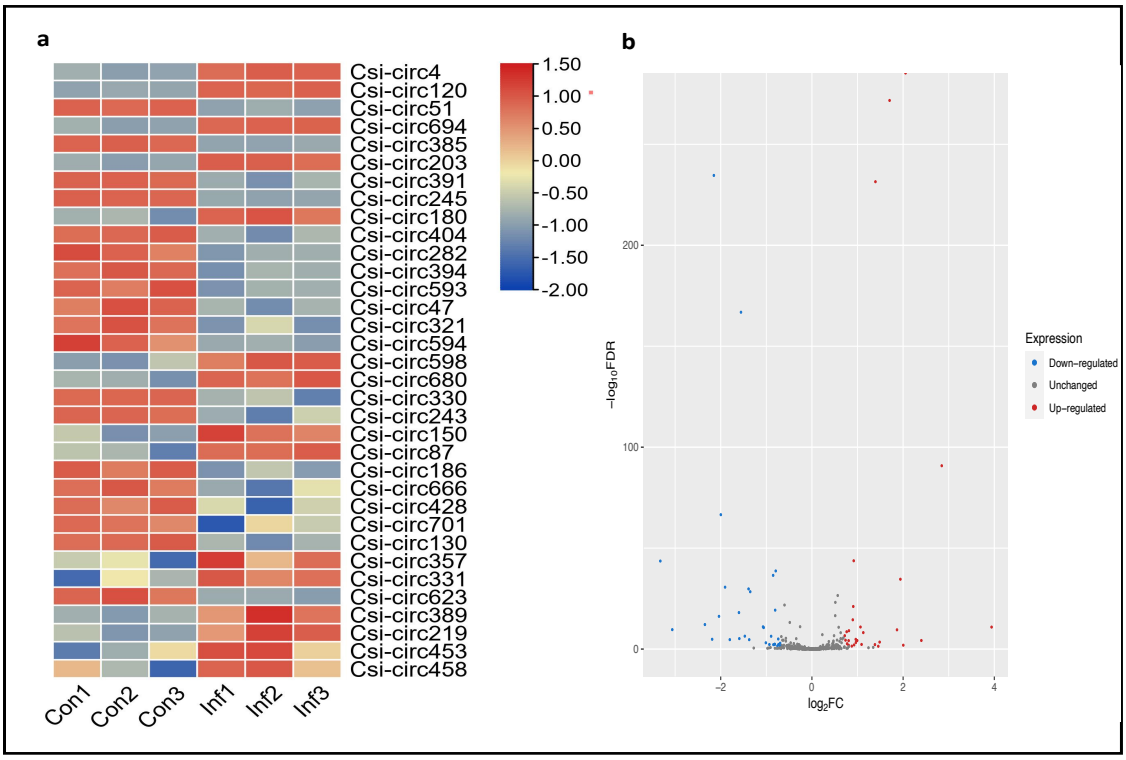

Fig. 4.34 Differential expression pattern of identified circRNAs. (a) A heatmap showing the expression pattern of DECs across all six samples (b) Volcano plot showing differential expression of circRNAs

4.6.3 Functional characterization of DECs

To establish the relationship of the identified circRNAs with protein coding genes of *C. sinensis* and to explore the biological processes in which the circRNAs are involved, we performed a circRNA-mRNA co-expression analysis. We applied a stringent cut-off of 0.9 for PCC (Bordoloi *et al*. 2021) to find out only highly co-expressing circRNA-mRNA pairs. We identified 3387 genes to be correlated with the expression pattern of the DECs. Functional characterization of the DEC parental genes and correlated genes revealed that the DEC-target genes were annotated under 407 GO terms, of which 322 were under "Biological Processes", 37 under "Cellular Component" and 48 GO terms were found to be under "Molecular function". The distribution of DEC-target genes under GO terms has been depicted in Fig. 4.35.

Table. 4.5 List of DECs annotated with their parental genes

DEC	**Parental gene id**	**Derived from**	**Parental gene information**
Csi-circ203	CSS0045875	exon	Alpha-terpineol synthase like
Csi-circ404	CSS0042855	exon	Shikimate dehydrogenase
Csi-circ593	CSS0007547	intron	U2 splicing factor large subunit
Csi-circ47	CSS0044326	exon	cdc protein
Csi-circ321	CSS0006029	exon	shikimate O-hydroxycinnamoyl
Csi-circ598	CSS0016268	exon	uncharacterized
Csi-circ87	CSS0027271	exon	Protein phosphatase

Csi-circ186	CSS0002159	intron	HEN4-like
Csi-circ666	CSS0041035	exon	uncharacterized
Csi-circ701	CSS0017612	exon	ser/thr protein phosphatase
Csi-circ357	CSS0000146	intron	F-box/WD40 repeat containing protein

Based on GSEA of KEGG pathway, it was found that the upregulated DEC-target genes are enriched in KEGG pathways such as “diterpenoid biosynthesis”, “nucleocytoplasmic transport”, “tryptophan metabolism”, “ascorbate and aldarate metabolism”, “biosynthesis of secondary metabolites” and “biosynthesis of cofactors”. Whereas downregulated DEC-target genes are enriched in “N-glycan biosynthesis” and “porphyrin metabolism” pathways. Fig. 4.36 depicts the KEGG annotation result output.

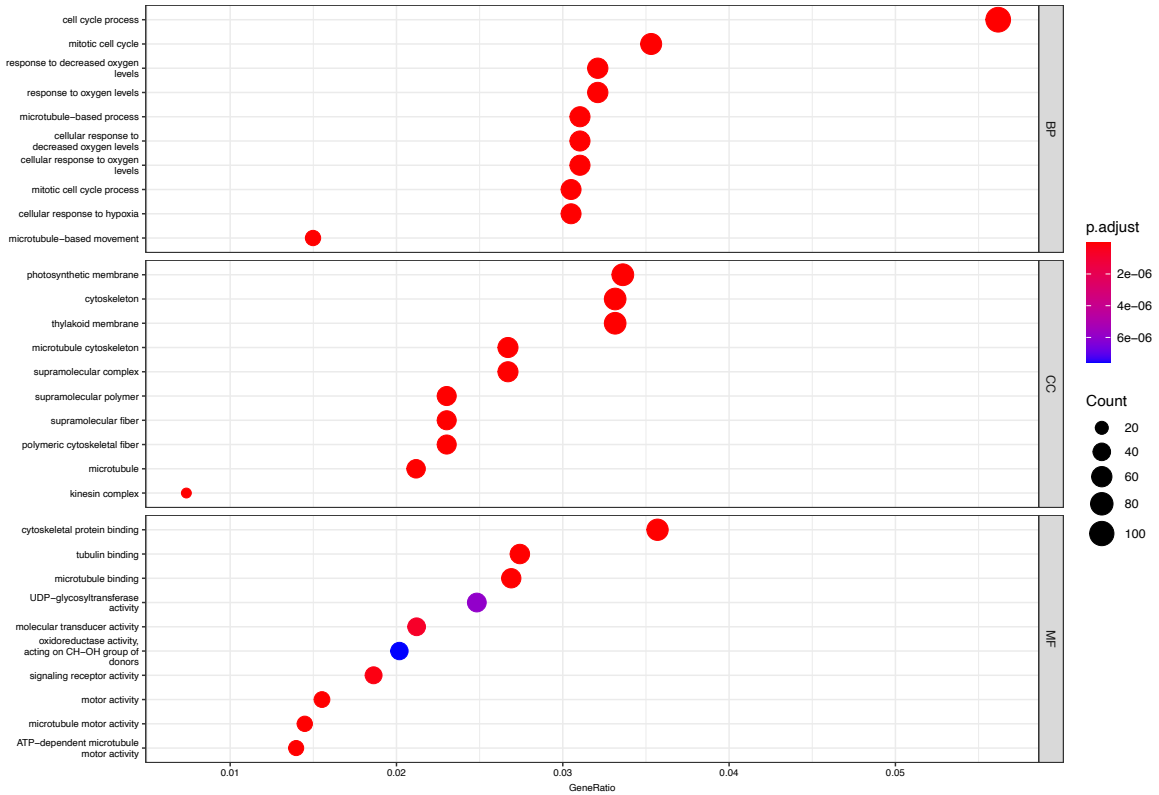

Fig. 4.35 Annotation of the DEC-target genes based on GO. The x-axis depicts the enrichment ratio between number of DEC-target genes and all UniGenes enriched in a particular GO term. The size of the bubble represents number of DEC-target genes assigned to the particular GO term and the color of the bubble represents adjusted p-value (q value). BP; Biological processes, CC; Cellular component, MF; Molecular function

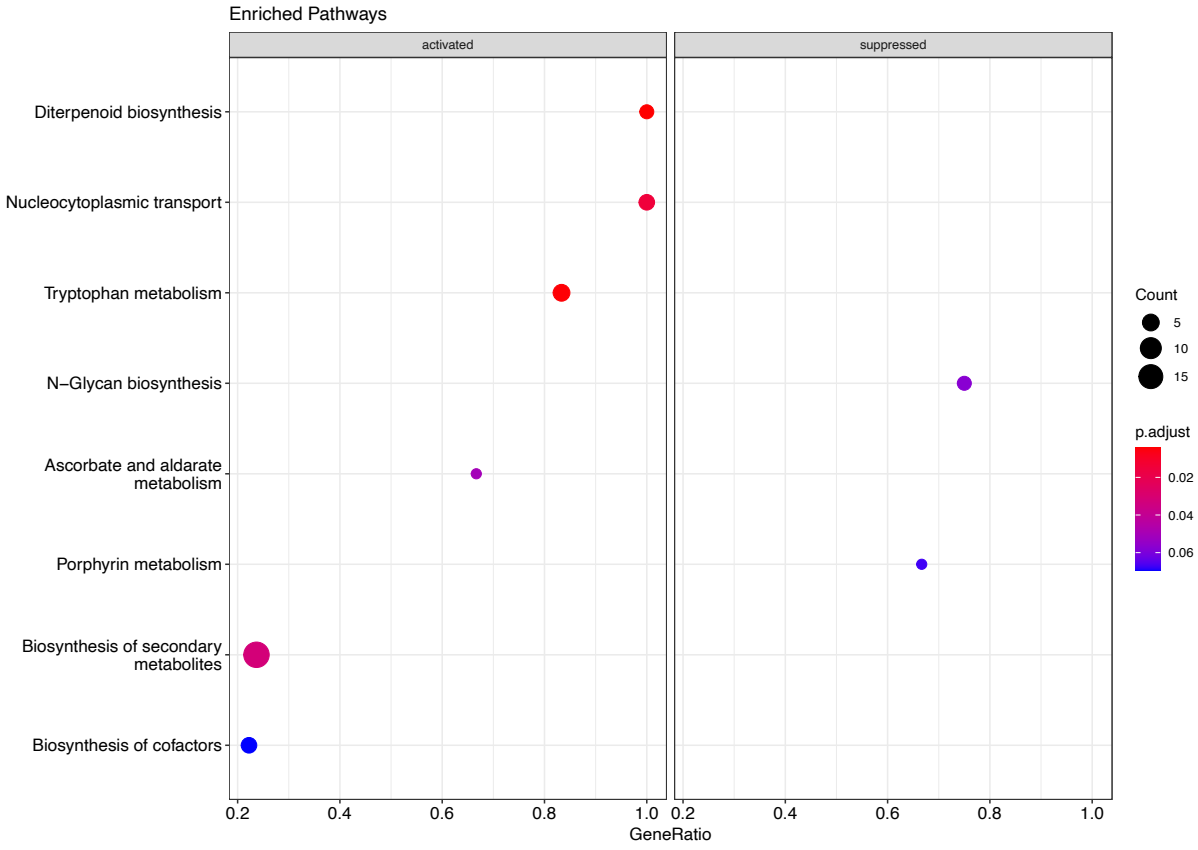

Fig. 4.36 GSEA based on KEGG pathway of DEC-target genes. The x-axis depicts the enrichment ratio between number of lncRNA-target genes and all UniGenes enriched in a particular KEGG pathway. The size of the bubble represents number of DEC-target genes assigned to the particular KEGG pathway and the color of the bubble represents adjusted p-value (q value). The left halve of the figure represents pathways upregulated in response to TMB and the right halve represents pathways downregulated in response to TMB.

4.7 miRNA targets, eTMs

LncRNAs can serve as potential miRNA targets to impart significant influence on miRNA active level. Therefore, it is necessary to assess the possibility of TMB-responsive lncRNAs that can effectively act as targets of conserved as well as novel *C. sinensis* miRNAs. A total of 28 DELs were identified to be potential targets of 46 *C. sinensis* miRNAs. Most of the miRNAs targeting the lncRNAs were novel to *C. sinensis*. A high frequency of miRNAs were seen to target five to twelve lncRNAs. Notably, conserved miRNAs like miR156, miR171 and miR395 were predicted to target 6 lncRNAs. These miRNAs are well-known to participate in plant-insect interaction (Stief *et al*. 2014; Wang *et al*. 2018) and hence, the lncRNAs targeted by these miRNAs might be potential candidates for regulation of gene expression during TMB stress in *C. sinensis*. TCONS_00099260 was targeted by as many as 12 miRNAs including the conserved miR171 and TCONS_00063108 is a potential target for 8 miRNAs novel to *C. sinensis.* Additionally, 7 lncRNAs were found to act as eTMs.

Table 4.6 Table showing lncRNAs acting as eTMs and the corresponding mRNAs with their available information

miRNA	**eTM**	**mRNA**	**mRNA information**
Csn-miR1310	TCONS_00028490	-	-
Csn-miR171	TCONS_00087056	CSS0048675	SCARECROW like protein
		CSS0048959	UDP-glycosyltransferase like
		CSS0045390	UDP-glycosyltransferase like

		CSS0043196	Replication protein
		CSS0005439	Glycine dehydrogenase
		CSS0037920	Glycine dehydrogenase
		CSS0045428	Polymerase IV like
		CSS0032383	Polymerase IV like
		CSS0016814	UDP-glycosyltransferase like
		CSS0036502	6,7-dimethyl-8-ribityllumazine synthase
Csn-miR2936	TCONS_00129063	-	-
Csn-miR5558	TCONS_00034064	-	-
Csn-miR6173	TCONS_00128571	-	-
Csn-miRn2	TCONS_00088006	CSS0028211	Dirigent protein like
	TCONS_00088007	CSS0044221	Dirigent protein like
		CSS0025659	TMV resistance protein like

Table 4.7 Table showing *C. sinensis* miRNAs targeting DELs

miRNA	Target	E-value	miRNA _start	miRNA _end	Target_start	Target_end	miRNA_aligned_fragment	Target_aligned_fragment	Inhibition
csn-miRn212	TCONS_00099260	1.5	1	24	204	227	UUGGAAAAGGAAAGGGAAAAUGUC	ACACCUUUUCCUUUCUUUUUUCAA	Cleavage
csn-miRn301	TCONS_00099260	2	1	24	205	228	UUUGGAAAUAGAAAGGAAAAAGAU	CACCUUUUCCUUUCUUUUUCAAA	Cleavage
csn-miRn82	TCONS_00099260	2	1	24	205	228	UUUGGAAAGAGAAAAGAAAAAGAC	CACCUUUUCCUUUCUUUUUCAAA	Cleavage
csn-miR4403	TCONS_00118970	2.5	1	24	2047	2070	ACGGACACCGGACACGACACGGAC	GUCCGUGUCAUGUCAGGUGUCCGU	Translation
csn-miRn144	TCONS_00030552	2.5	1	24	457	480	GAAUGGAUUUAAAAAGAAAAAGGA	UGCAGUUUCAUUUUAAAUCUGUUU	Cleavage
csn-miRn144	TCONS_00030553	2.5	1	24	444	467	GAAUGGAUUUAAAAAGAAAAAGGA	UGCAGUUUCAUUUUAAAUCUGUUU	Cleavage
csn-miRn154	TCONS_00099260	2.5	1	24	205	228	UUUGAAAAGGGAAAUGGAAAACAU	CACCUUUUCCUUUCUUUUUCAAA	Cleavage
csn-miRn231	TCONS_00022462	2.5	1	23	1702	1724	UGCAUCUAUAGCUGUGAACAAUU	UUGUGUUUAAAGCUAUGGAUGUA	Cleavage
csn-miRn37-3p	TCONS_00022462	2.5	1	23	1702	1724	UGCAUCUAUAGCUGUGAACAAUU	UUGUGUUUAAAGCUAUGGAUGUA	Cleavage
csn-miRn431	TCONS_00114397	2.5	1	24	312	335	AACCACACAAUGUAGUACUCUAGG	UUUGAUGUACUAAAUUGUGUGGUU	Cleavage

csn-miRn51	TCONS_0009 9260	2.5	1	24	210	233	AGUGAUUUGGAAAAC GAAAGAGAA	UUUCCUUUCUUUUU UCAAAUUAUU	Cleavage
csn-miRn52-3p	TCONS_0009 6802	2.5	1	21	37	57	CGUUGGAAGUCUUUG AGGGUA	GCCCCUCAGAGACUU UCAAUC	Cleavage
csn-miRn58-5p	TCONS_0009 9260	2.5	1	21	232	252	UUGGCUCAUGGAUUU GGGGAG	UUUUCCAAAUCCAU GAACCAA	Cleavage
csn-miR395h	TCONS_0009 6174	3	1	21	240	260	GUUCCUCUGAACACUU CAUUG	UGAAGAAGUGUUUG GAGGAAA	Cleavage
csn-miRn164	TCONS_0011 5148	3	1	24	471	494	UUUCGUAACUCAAAUU UUGUGGCU	AAAGAGAAAAUUUG AUUUGCGAAA	Cleavage
csn-miRn212	TCONS_0006 3108	3	1	24	102	125	UUGGAAAAGGAAAGG GAAAAUGUC	GACAAUUUUCUUUU CUUUUUUUAG	Cleavage
csn-miRn239	TCONS_0009 9260	3	1	24	207	229	AUUUGGAAAAGGAAA UGGAAAAGC	CCUUUUCC-UUUCUUUUUUCAAA	Cleavage
csn-miRn278	TCONS_0009 9260	3	1	24	114	137	AGAAAUUUCGUCAAAC UCAGAGAA	GUUUAUGGAUUUGA UGAGAUUUUU	Cleavage
csn-miRn311	TCONS_0011 4397	3	1	24	404	427	AACUAGAAACACGAGA ACAAUCGC	UUUUUUGUUCUGGU UUUUCUAGUU	Translation
csn-miRn335	TCONS_0009 6174	3	1	24	419	442	GAAAGGAAAAUGAAA AAAGUAGGU	UUUUUUUUUUUUUU UUUUCUUUUC	Translation
csn-miRn421	TCONS_0006 3108	3	1	24	102	125	UUUAGAAAGGAAAAG AAAAAAGAU	GACAAUUUUCUUUU CUUUUUUUAG	Cleavage
csn-miRn57	TCONS_0011 5148	3	1	24	394	417	AGAGAUUUGGAAAAG GAAAUGAAA	UAAAAUUUUUUUUU UCUAAUCUCU	Cleavage

csn-miRn82	TCONS_00063108	3	1	24	103	126	UUUGGAAAGAGAAAAGAAAAAGAC	ACAAUUUUCUUUUCUUUUUUUAGU	Cleavage
csn-miR156c-3p	TCONS_00083891	3.5	1	22	215	236	GCUCACUUCUCUUUCUGUCAUU	AGAGAAAGGGAGAGAAAUGAGC	Cleavage
csn-miR156h	TCONS_00053665	3.5	1	21	226	246	UGACAGAAGAGAGAGAGCACA	AUAGCUCUCUCUCUUCUCUCU	Cleavage
csn-miR156h	TCONS_00053665	3.5	1	21	226	246	UGACAGAAGAGAGAGAGCACA	AUAGCUCUCUCUCUUCUCUCU	Cleavage
csn-miR166b-5p	TCONS_00040585	3.5	1	21	1001	1021	GAAUGUCGUCUGGUUCGAAAU	UUUUCUAUCCAGAUGAUAUUU	Cleavage
csn-miR171q	TCONS_00099260	3.5	1	24	823	846	UUGAUUUGAUUGAGCCGCGCCAAU	GGUUAGGCAGCCCAAUCAAAUCAA	Cleavage
csn-miR395h	TCONS_00108694	3.5	1	21	31	51	GUUCCUCUGAACACUUCAUUG	GAAUCAAAUGUUUGGAGGGAC	Cleavage
csn-miR828	TCONS_00001085	3.5	1	22	459	480	UCUUGCUCAAAUGAGUAUUCCA	CCGAUUUUUUAUUUGAGUAAGA	Cleavage
csn-miR828a	TCONS_00001085	3.5	1	22	459	480	UCUUGCUCAAAUGAGUAUUCCA	CCGAUUUUUUAUUUGAGUAAGA	Cleavage
csn-miRn120	TCONS_00038780	3.5	1	24	866	889	GUAAAGUACAUGGACCAAAUUGAC	GAACAUUUGGGUGAUGUACUUUGC	Cleavage
csn-miRn125	TCONS_00032354	3.5	1	24	267	290	AAUGAGAUUUUGACUGAUAGAAGU	AUGGAUAUUGGUUAGAGUUUUAUU	Cleavage
csn-miRn13	TCONS_00022462	3.5	1	24	1715	1738	CAUCUAUGAAUCGGUACAUUUGAC	UAUGGAUGUAUCUAUACAUAGAUG	Cleavage

csn-miRn171	TCONS_0006 2765	3.5	1	24	165	188	AUUUCGUCCAAUUAUU AACAGAAU	CAAGAGUUGUUGAU UGGACGAAGG	Cleavage
csn-miRn192-3P	TCONS_0011 4397	3.5	1	24	310	334	ACCACACAAUGUAGUA C-UCGAGGA	CAUUUGAUGUACUA AAUUGUGUGGU	Translation
csn-miRn212	TCONS_0000 1085	3.5	1	24	319	342	UUGGAAAAGGAAAGG GAAAAUGUC	UUGUUUUUACUUUU UCUUUUUUAG	Cleavage
csn-miRn260	TCONS_0011 4397	3.5	1	21	317	337	UCAAGCACACAAUGUA GUACU	UGUACUAAAUUGUG UGGUUGU	Cleavage
csn-miRn292	TCONS_0011 4397	3.5	1	24	403	426	ACUAGAAGAACCAAAU UGACACAU	AUUUUUUGUUCUGG UUUUUCUAGU	Cleavage
csn-miRn32-3p	TCONS_0011 4397	3.5	1	24	310	334	ACCACACAAUGUAGUA C-UCGAGGA	CAUUUGAUGUACUA AAUUGUGUGGU	Translation
csn-miRn33	TCONS_0010 6979	3.5	1	24	213	236	AGCACCUGUCAACAAU UUCUUACC	CUUUCACAGUUGUU GGCAGGUGUU	Cleavage
csn-miRn340	TCONS_0002 2462	3.5	1	24	2361	2384	AAAUGACAAUUUUAC UCCUUUCGA	GAUGGAUGGGUAAG AUUGUCAAUU	Cleavage
csn-miRn358	TCONS_0001 7587	3.5	1	24	1272	1295	AGGAAACUUUAGGGA AAAAUCACU	UAUUUUUUUUUGUU AGGGUUUCCU	Cleavage
csn-miRn377	TCONS_0007 7127	3.5	1	24	59	82	AUUUGAUGAGAGAUU UGGAAAUGA	CUAUCUCCGAAUUUC UCUUUGAAU	Cleavage
csn-miRn377	TCONS_0012 4553	3.5	1	24	1510	1533	AUUUGAUGAGAGAUU UGGAAAUGA	AUCUGUUCAAAUUU UUUAUCAUAU	Cleavage
csn-miRn383	TCONS_0002 4800	3.5	1	24	102	125	AUUUGAGAAAUUACA GAUACUCCC	GGGUGUAUUUGUAA UUUAUCAAUU	Cleavage

csn-miRn402	TCONS_00072135	3.5	1	24	202	224	AAUAAAUCUCAACCAUACACUGUA	ACCUCUGUAUGGU-GAGAUUUGUU	Translation
csn-miRn41	TCONS_00114397	3.5	1	21	317	337	UCAAGCACACAAUGUAGUACU	UGUACUAAAUUGUGUGGUUGU	Cleavage
csn-miRn421	TCONS_00114397	3.5	1	24	229	252	UUUAGAAAGGAAAAGAAAAAAGAU	UUCUUUUUUUUCUUUUUUUCUGAA	Cleavage
csn-miRn421	TCONS_00021732	3.5	1	24	524	547	UUUAGAAAGGAAAAGAAAAAAGAU	GGUUUUUUUUUUUUUUUUUAGU	Cleavage
csn-miRn424	TCONS_00017587	3.5	1	24	1272	1295	AGGAAACUUUAGAGAAAAAUCACU	UAUUUUUUUUUGUUAGGGUUUCCU	Cleavage
csn-miRn428	TCONS_00096802	3.5	1	24	504	527	AAUUGGUUAUACUAGGAAUUAGUG	CUCUGGUUUUUUGUAUGACCAAUU	Cleavage
csn-miRn446	TCONS_00025347	3.5	1	24	1540	1563	AGAAGAGAAUGUAUUUGAAACAAA	UCCUCCUUAAAUAUGUUUUCUUUU	Cleavage
csn-miRn446	TCONS_00024234	3.5	1	24	1492	1515	AGAAGAGAAUGUAUUUGAAACAAA	UCCUCCUUAAAUAUGUUUUCUUUU	Cleavage
csn-miRn478	TCONS_00118970	3.5	1	24	624	647	AAAGGUGAGGCUUGAGGUCCUACU	UGAUACUCUUCAAGCCUUGCCUUU	Cleavage
csn-miRn57	TCONS_00099260	3.5	1	24	210	233	AGAGAUUUGGAAAAGGAAAUGAAA	UUUCCUUUCUUUUUUCAAAUUAUU	Cleavage
csn-miRn58	TCONS_00034064	3.5	1	24	1194	1217	AUGGACCAAAUUGACACAUCAUGU	UCUUUAUCUUUUGGUUUGGUCCAU	Cleavage
csn-miRn7	TCONS_00099260	3.5	1	24	102	125	AAAUUCUUGAACCAAAUGCAGCCU	CCAUGGUGUUUGGUUUAUGGAUUU	Cleavage

csn-miRn90-3P	TCONS_0011 4397	3.5	1	24	386	409	AAAAAAUCCUAUUAU GACUCCUCG	ACGCUCAUCAAAAU GGGAUUUUUU	Cleavage
csn-miRn99	TCONS_0009 9260	3.5	1	24	1424	1447	AUAAAUGUGAGUCGA UGAAAGGGU	AACCAUUUGUUAAU UCACAUUUAU	Cleavage
csn-miR156c	TCONS_0003 2903	4	1	21	544	564	UUGACAGAAGAAAGA GAGCAC	UUGGACUAUUUUUU UUGUCAA	Cleavage
csn-miR156e	TCONS_0003 2903	4	1	21	544	564	UUGACAGAAGAAAGA GAGCAC	UUGGACUAUUUUUU UUGUCAA	Cleavage
csn-miR156f	TCONS_0011 6642	4	1	22	193	214	UGCUCACUUCUCUUCU GUCAGC	AAUGAAACAACAGA GGUGAGCA	Cleavage
csn-miR166a-5p	TCONS_0004 0585	4	1	21	1002	1022	GGAAUGUCGUCUGGU UCGAAA	UUUCUAUCCAGAUG AUAUUUU	Cleavage
csn-miR166d	TCONS_0004 0585	4	1	21	1002	1022	AGAAUGUUGUCUGGC UCGAGG	UUUCUAUCCAGAUG AUAUUUU	Cleavage
csn-miR166e	TCONS_0004 0585	4	1	21	1002	1022	GGAAUGUUAUCUGGC UCGAGG	UUUCUAUCCAGAUG AUAUUUU	Cleavage
csn-miR166k	TCONS_0004 0585	4	1	21	1002	1022	GGAAUGUCGUCUGGU UCGAAA	UUUCUAUCCAGAUG AUAUUUU	Cleavage
csn-miR5368e	TCONS_0009 6174	4	1	20	439	458	AGAUACCACUCUGGAA GAGC	UUUCUUUUAGGGUU GUAUUU	Cleavage
csn-miR6300b	TCONS_0006 2765	4	1	21	394	414	GUUGUAGUAUAGUGG UGAGUA	CACUGAUUAUUAUA UUAUAAU	Cleavage
csn-miRn107	TCONS_0008 7056	4	1	24	1119	1142	AUUCAGUAGAAAAUU UGGUAUCCC	CAGGUGAGGAAUUU UUUAUUGAAU	Cleavage

csn-miRn107	TCONS_00038780	4	1	24	253	276	AUUCAGUAGAAAAUUUGGUAUCCC	AUAUUAUCGUGUUUUUUAUUGAGU	Cleavage
csn-miRn132-3P	TCONS_00024800	4	1	24	211	234	UAACCUGAGAACCAACAUUGCGAG	AGUACAAUGUUGGUUCUUGAUUUA	Cleavage
csn-miRn144	TCONS_00078068	4	1	24	413	436	GAAUGGAUUUAAAAAGAAAAAGGA	AUGAUUUUUUUUUUAAUUCCUUUU	Cleavage
csn-miRn146	TCONS_00025347	4	1	24	969	992	AAGAGAUUUAGAAAAGAAAAAGAA	ACUUUUUUUAUUUUUAAAUUUUUA	Cleavage
csn-miRn146	TCONS_00024234	4	1	24	921	944	AAGAGAUUUAGAAAAGAAAAAGAA	ACUUUUUUUAUUUUUAAAUUUUUA	Cleavage
csn-miRn146	TCONS_00017587	4	1	24	367	390	AAGAGAUUUAGAAAAGAAAAAGAA	UGUUCUUUUUUUACUAAAUUUUUC	Cleavage
csn-miRn154	TCONS_00069554	4	1	24	288	311	UUUGAAAAGGGAAAUGGAAAACAU	ACCUUCUUCAUUUCUCUUUUUUAA	Cleavage
csn-miRn162	TCONS_00078068	4	1	24	411	434	GAGGAUUUGAAAAGAAAUUUGAAA	AUAUGAUUUUUUUUUUAAUUCCUU	Cleavage
csn-miRn17	TCONS_00118970	4	1	21	1458	1478	GUGCUGUCUAUCGUCGUCAUG	CUUGACGGAGAUAGAUAGUAG	Cleavage
csn-miRn172	TCONS_00115148	4	1	24	238	261	AGUGAAAGAAAAAAGGUAUGUGAA	UUCACAGGCCUUUUUUUUUUAAU	Cleavage
csn-miRn172	TCONS_00053665	4	1	24	247	270	AGUGAAAGAAAAAAGGUAUGUGAA	CUUCCAUUUCCUUUUUGUUUCACU	Cleavage
csn-miRn192-5P	TCONS_00118970	4	1	21	544	564	UUUCUAGAGUACUACAUUGUG	UUCCAUUUAUUACUUUAGAAA	Cleavage

csn-miRn203	TCONS_00115148	4	1	24	536	559	UAAUCGGAAUACAUUUUUGUCAAU	UGUUUUGAAACUGUAUGCUGAUUA	Cleavage
csn-miRn205-5P	TCONS_00096174	4	1	25	440	464	UGGCUCAAAUGUGGCUCAAAUGGCU	UUCUUUUAGGGUUGUAUUUGAGUCA	Cleavage
csn-miRn207	TCONS_00034064	4	1	24	852	875	AUAAAUUUUAACCAGUAGCAUAAC	CUUUAGCUAUUGGUUGAAAAUUGA	Cleavage
csn-miRn212	TCONS_00115148	4	1	24	736	759	UUGGAAAAGGAAAGGGAAAAUGUC	CUUUACUUUUUUUUUUUUUCAA	Cleavage
csn-miRn212	TCONS_00021732	4	1	24	523	546	UUGGAAAAGGAAAGGGAAAAUGUC	UGGUUUUUUUUUUUUUUUUAG	Cleavage
csn-miRn214	TCONS_00087056	4	1	24	8	31	ACCCGAGUGAGACAUUUGAUCAUU	GGGGCUAAAAAGUCUCAUUUGGGA	Cleavage
csn-miRn219	TCONS_00032903	4	1	24	233	256	ACAAUUGGACGGAAUGUGUUGAUG	GAAAAAUAUGAUUUGUCUAAUUGU	Cleavage
csn-miRn221	TCONS_00068537	4	1	24	647	670	AAAUUUAUGAUCAUUGGAUUACCU	GAUUUAUAUAUUGAUUAUAGGUUU	Cleavage
csn-miRn222	TCONS_00017587	4	1	24	1165	1188	AUCCGAUAGACAUGAUUUUUUACA	UAAGUAGAAGCAUGUUUGUGGGAU	Cleavage
csn-miRn239	TCONS_00115148	4	1	24	94	117	AUUUGGAAAAGGAAAUGGAAAAGC	CCCAGUUCAUUUUCUUUUACAAUU	Cleavage
csn-miRn241	TCONS_00099260	4	1	24	271	294	AUUGAUCGGAUAUCGAUAGUAACU	GAUGUCUAUAGAUAUCUAAUCAAA	Cleavage
csn-miRn261	TCONS_00032354	4	1	24	1031	1054	GAAACGGAAAAGAUGUGUGAAACU	UGUUGAGUACAUUUUUUCCUUUUC	Cleavage

csn-miRn268	TCONS_00025347	4	1	24	969	992	GAGGAAUUUGAAAAGGAAAAGUGA	ACUUUUUUUAUUUUUAAAUUUUUA	Cleavage
csn-miRn268	TCONS_00024234	4	1	24	921	944	GAGGAAUUUGAAAAGGAAAAGUGA	ACUUUUUUUAUUUUUAAAUUUUUA	Cleavage
csn-miRn268	TCONS_00115148	4	1	24	98	121	GAGGAAUUUGAAAAGGAAAAGUGA	GUUCAUUUUCUUUUACAAUUCUUC	Translation
csn-miRn27	TCONS_00078068	4	1	24	443	466	ACUGUUUUGAGCCAUUGUGACCAC	CUUCUCACAGUCGUUCAAAAAAGU	Cleavage
csn-miRn27	TCONS_00088006	4	1	24	150	173	ACUGUUUUGAGCCAUUGUGACCAC	ACAUAUGCAUUGGCUUGAAGUAGU	Cleavage
csn-miRn278	TCONS_00124553	4	1	24	1014	1037	AGAAAUUUCGUCAAACUCAGAGAA	GACAAUUAAUAUGAUGAAAUUUUU	Cleavage
csn-miRn290	TCONS_00099260	4	1	24	287	310	AUGUGUAAAAAGUGUAUUAAAAUA	UAAUCAAAUUAAUUUUUUACAUAU	Cleavage
csn-miRn292	TCONS_00118970	4	1	24	1045	1068	ACUAGAAGAACCAAAUUGACACAU	UAAAGUAGAUUUGGUUUUUUUAAU	Cleavage
csn-miRn294	TCONS_00104371	4	1	24	115	138	UUGAGCCAUUGUAGCCACAAAAAU	AGAACUUUGGCUUCAAUGGAUCAA	Cleavage
csn-miRn30	TCONS_00116642	4	1	24	114	137	AGUGGAUGAAAGGAUAAACGAUAU	UUGUUGUUUGCUCUUUCAUUCCCU	Cleavage
csn-miRn301	TCONS_00021732	4	1	24	384	407	UUUGGAAAUAGAAAGGAAAAAGAU	GUUUUUUUUUUUUUUGUUUUUAAU	Cleavage
csn-miRn301	TCONS_00096174	4	1	24	546	569	UUUGGAAAUAGAAAGGAAAAAGAU	UGUAAUUUUAUUUUUAUUUCUUAA	Cleavage

csn-miRn307	TCONS_00040585	4	1	24	1032	1055	GUUAUUGGAUGGGGAUACCACGUG	GUAACUAUAUGCUCAUCCAAUAAU	Cleavage
csn-miRn31	TCONS_00132530	4	1	24	217	240	ACUUUUAGUAGAAUUUUUGGGGCC	CACUUCAUCAAUUCUAAUAAAGGU	Cleavage
csn-miRn315	TCONS_00040585	4	1	24	227	250	GAAAGAAUUAUGAUCAUUGGAUUA	CUUCUUAAUGAUUUUGAUUUUUUU	Translation
csn-miRn32-5p	TCONS_00118970	4	1	21	544	564	UUUCUAGAGUACUACAUUGUG	UUCCAUUUAUUACUUUAGAAA	Cleavage
csn-miRn322	TCONS_00072135	4	1	24	202	224	GAUAAAUCUCAACCAUACACUGUA	ACCUCUGUAUGGU-GAGAUUUGUU	Translation
csn-miRn328	TCONS_00072135	4	1	24	202	224	AGUAAAUCUCAACCAUACACUGUA	ACCUCUGUAUGGU-GAGAUUUGUU	Translation
csn-miRn331	TCONS_00088007	4	1	24	290	313	AUGAUCAUGAAAGAUUUGUAACCU	CAUGAAUGGAUCUUUCAUGUUCAA	Cleavage
csn-miRn340	TCONS_00096174	4	1	24	530	553	AAAUGACAAUUUUACUCCUUUCGA	CUUAGUUGGGUAAAAUUGUAAUUU	Cleavage
csn-miRn346	TCONS_00022462	4	1	24	358	381	AAGUUGAUCGGCUAUCAAUAACCU	GUUGAAUUGAUGGUGGAUCAAAUU	Translation
csn-miRn358	TCONS_00017587	4	1	24	368	391	AGGAAACUUUAGGGAAAAAUCACU	GUUCUUUUUUUACUAAAUUUUUCU	Cleavage
csn-miRn392	TCONS_00096174	4	1	24	546	569	UUUAGAAAGAGAAAUAGAAAAGGU	UGUAAUUUUAUUUUUAUUUCUUAA	Cleavage
csn-miRn397	TCONS_00077127	4	1	24	62	85	AGGAUUUGAGGAGAGAUUUAGAAA	UCUCCGAAUUUCUCUUUGAAUCUG	Cleavage

csn-miRn397	TCONS_00099260	4	1	24	308	331	AGGAUUUGAGGAGAGAUUUAGAAA	UAUGUAUUUUUCUCUUCGAGUCCU	Cleavage
csn-miRn411	TCONS_00115148	4	1	23	396	418	AAGAGAUUUGGAAAGGAAAACGG	AAAUUUUUUUUUUCUAAUCUCUC	Cleavage
csn-miRn416	TCONS_00034064	4	1	24	1302	1325	AAGAGUUAUGAUCAUUGGAUUACC	UCUAAUUUGAACAUCAUAACUCUU	Cleavage
csn-miRn421	TCONS_00021732	4	1	24	384	407	UUUAGAAAGGAAAAGAAAAAAGAU	GUUUUUUUUUUUUUUGUUUUUUAAU	Cleavage
csn-miRn421	TCONS_00001085	4	1	24	319	342	UUUAGAAAGGAAAAGAAAAAAGAU	UUGUUUUUACUUUUUCUUUUUUUAG	Cleavage
csn-miRn424	TCONS_00017587	4	1	24	368	391	AGGAAACUUUAGAGAAAAAUCACU	GUUCUUUUUUUACUAAAUUUUUCU	Cleavage
csn-miRn43	TCONS_00099260	4	1	24	1001	1024	AGUUGAUCGGAUAUCAAUAGACCU	CGCCUUAUGGAUGUCCGAAUGACU	Cleavage
csn-miRn433	TCONS_00088007	4	1	24	441	464	AACAAAUGUGAGAUCUUGGACCCA	GUGGAUUGAAAUGUCACAUUUGUU	Cleavage
csn-miRn433	TCONS_00015431	4	1	24	670	693	AACAAAUGUGAGAUCUUGGACCCA	CUUUUUCAUGAUUUUACAUUUUUU	Cleavage
csn-miRn441	TCONS_00024800	4	1	24	871	894	AGAGAAUGAGACAAAUGAUUUAUA	CCUAUGUUACUUGUUUUAUUUUUU	Cleavage
csn-miRn45	TCONS_00040585	4	1	24	1642	1665	AUGUAACUUGCCAAUAAAUCUCAA	CCUCAAUUUCUUGGCUAGAUACAU	Cleavage
csn-miRn461	TCONS_00118970	4	1	24	39	62	GUUUUGUGACCCUUGAAUUACACU	GUACAAAAUUAGGGGUGGCAAAAC	Cleavage

csn-miRn465-3P	TCONS_00068537	4	1	24	1545	1568	UUGAGAUUCAUUUGUGGCAUGGUC	AUUGAUGCAAGAAAUGAAUUUGAA	Cleavage
csn-miRn469	TCONS_00114397	4	1	24	310	333	CCACACAAUGUAGUACUCUAGGAA	CAUUUGAUGUACUAAAUUGUGUGG	Translation
csn-miRn47	TCONS_00124553	4	1	23	844	866	AAGAUUUGGAAAGGGAAAUGAAA	AUUUAAUUUCAUUUUCAAAUUUU	Cleavage
csn-miRn48	TCONS_00072135	4	1	24	202	224	AGUAAAUCUCAACCAUACACUGUA	ACCUCUGUAUGGU-GAGAUUUGUU	Translation
csn-miRn49	TCONS_00024800	4	1	21	875	895	CAGAGAGUGAAACAGAUGAUC	UGUUACUUGUUUUAUUUUUUG	Cleavage
csn-miRn64	TCONS_00025819	4	1	24	257	280	ACGAGCAAUGUUUUAUAGAAGAUC	AUAAUGCAACAAGACAUUGCUUGU	Cleavage
csn-miRn68	TCONS_00118970	4	1	21	1458	1478	GUGCUGUCUAUCGUCGUCAUG	CUUGACGGAGAUAGAUAGUAG	Cleavage
csn-miRn75	TCONS_00143159	4	1	24	513	536	AAACAAGUUACAAUUGUCGGACCC	AUGGUGGGCGAUUGUAAUUUUUUUU	Cleavage
csn-miRn76	TCONS_00068537	4	1	24	1193	1216	AAAUAUUAUAAUUAUUAGAUCGAA	AAUUAAUUGGUGAUUGUAAUGUUU	Cleavage
csn-miRn82	TCONS_00114397	4	1	24	229	252	UUUGGAAAGAGAAAAGAAAAAGAC	UUCUUUUUUUUCUUUUUUCUGAA	Cleavage
csn-miRn82	TCONS_00115148	4	1	24	742	765	UUUGGAAAGAGAAAAGAAAAAGAC	UUUUUUUUUUUUUUUCAAUCCAAA	Cleavage
csn-miRn82	TCONS_00022462	4	1	24	1816	1839	UUUGGAAAGAGAAAAGAAAAAGAC	UUGUUCUUCUCUUCUCUUUAUAAA	Cleavage

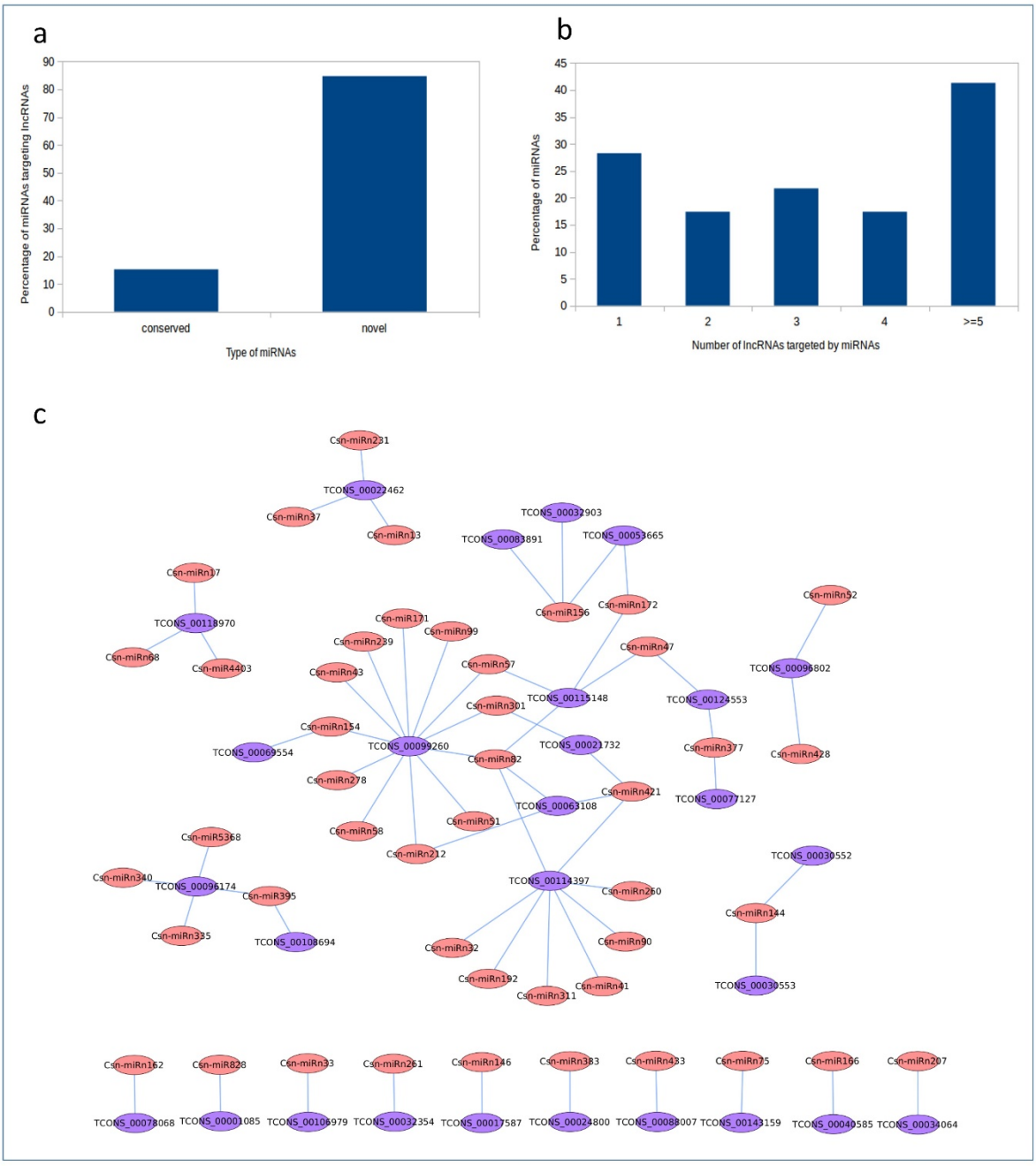

Fig. 4.37 (a) Percentage of novel and conserved *C. sinensis* miRNAs putatively targeting DELs (b) Percentage of miRNAs targeting on DELs (c) Interactive networks of *C. sinensis* miRNAs and DELs represented by pink and purple ellipse nodes respectively. The connection between miRNAs and lncRNAs are shown as blue edges.

```
>csn-miR1310a    Score: 4          TCONS_00028490
                            v  v
Query:             1 AACTTTAAAT--A-GGTAGG 17
                     ||||::||||   | |||o||
Sbjct:           390 TTGAGGTTTAGGTACCAGCC 371

>csn-miR171c     Score: 4          TCONS_00087056
                            v    v
Query:             1 TTGAGCCGTG---CCAATATCGC 20
                     |||||||:::    ||||o||||||
Sbjct:           917 AACTCGGTGTTTAGGTTTTAGCG 895

>csn-miR2936     Score: 4          TCONS_00129063
                            v  v
Query:             1 AGAGAGAGAA--C-ACAGAG 17
                     |||||||||o|   | ||o|||
Sbjct:            33 TCTCTCTCATCGGCTGACTC 14

>csn-miR5558     Score: 3.5        TCONS_00034064
                            v    v
Query:             1 TTTAGAATTA---GAATAGC 17
                     ||:|||||||    |||o|:o
Sbjct:           330 AAGTCTTAATTTCCTTTTTA 311

>csn-miR6173     Score: 3.5        TCONS_00128571
                            v    v
Query:             1 AAAGCTAGGG---GAGCGAA 17
                     |||||:||:|    ||||:o|
Sbjct:           158 TTTCGGTCTCAGACTCGTAT 139

>csn-miRn2       Score: 3          TCONS_00088006
                            v    v
Query:             1 ATTCCTACTG---GATGCACCA 19
                     |:|||:||||    |||o||||||
Sbjct:            45 TGAGGGTGACAAACTAAGTGGT 24
```

Fig. 4.38 Result of the lncRNA mimic analysis. Query signifies miRNA and Subject signifies lncRNAs. Score determines the expectation threshold; Dash (-) determines bulge formation.

```
>csn-miR156h    Score: 2.5      TCONS_00129063

Query:             1 TGACAGAAGAGAGAGAGCACA 21
                     *||*|||||||||||||*|*|
Sbjct:            54 TCTCTCTTCTCTCTCTC-TCT 35


>csn-miR156h    Score: 2.5      TCONS_00053665

Query:             1 TGACAGAAGAGAGAGAGC-ACA 21
                     *||*|||||||||||||*|*|
Sbjct:           246 TCTCTCTTCTCTCTCTCGATAT 225


>csn-miR156h    Score: 2.5      TCONS_00129063

Query:             1 TGACAGAAGAGAGAGAGCACA 21
                     *||*|||||||||||||*|*|
Sbjct:            54 TCTCTCTTCTCTCTCTC-TCT 35


>csn-miR156h    Score: 2.5      TCONS_00053665

Query:             1 TGACAGAAGAGAGAGAGC-ACA 21
                     *||*|||||||||||||*|*|
Sbjct:           246 TCTCTCTTCTCTCTCTCGATAT 225
```

Fig. 4.39 miRNA targeting lncRNA analysis through psRobot_tar; Score depicts the expectation threshold; Query determines the miRNA and subject determines the lncRNA; Asterisks (*) determine unpaired regions.

Previous high-throughput *in silico* assays have reported the post-transcriptional gene regulation by lncRNAs acting as ceRNAs that competitively block the interaction between miRNAs and target mRNAs (Fu *et al*. 2019; He *et al*. 2019; Zhou *et al*. 2020; Han *et al*. 2021). Assessment of the miRNA-lncRNA-mRNA interactome was performed for DELs and DEGs identified from untreated and TMB-treated samples. First, RNA-hybrid formation between miRNA-DEL and miRNA-DEG pairs were assessed, followed by cross-checking the presence of common miRNAs in both the datasets. Finally, DELs and DEGs sharing same miRNA were considered and fetched into Cytoscape for miRNA-lncRNA-mRNA network construction. The miRNA-lncRNA-mRNA network comprised of 28 miRNAs, 11 DELs and 14 DEGs. Interestingly, it was found that 7 miRNAs belonging to the family of miR156 target 3 DELs TCONS_00083891, TCONS_00053665 and TCONS_00032903 and 6 DEGs. These DEGs code for SPL (Squamosa promoter binding like) transcription factors that regulate phase transition and plant development, and pentatricopeptide repeat containing protein (PPR protein) that are characterized by the presence of tandem repeats of degenerate 30-35 amino acid residues. Previous reports suggest that the conserved miR156 targets SPL transcription factors and the miR156-SPL module has been widely investigated and studied in relation to plant development and stress response (Jeyakumar *et al*. 2020; Bordoloi and Agarwala, 2021). Also, PPR proteins are reported to be induced in response to various abiotic/biotic stimuli (Chen *et al*. 2018; Xing *et al*. 2018). The conserved miR171 targets TCONS_00099260 and 2 DEGs that code for a PPR protein and a GRAS family transcription factor. The involvement of GRAS family transcription factors in plant growth and development and insect stress response is well studied (Grimplet *et al*. 2016; Bordoloi and Agarwala, 2021). Other conserved miRNAs viz. miR395, miR5368, miR473, miR477, miR166 and

miR4403 form network with 5 DELs and 5 DEGs. These DEGs represent aspartyl proteases, DELLA proteins and homeodomain leucine zipper proteins (HD-Zip). HD-Zip proteins consist of a characteristic DNA-binding domain that regulate various plant developmental processes is response to altered environmental conditions (Zahur *et al*. 2013). Reports of the involvement of DELLA proteins in the jasmonic acid (JA) and gibberellic acid (GA) crosstalk suggest the important role of these growth repressors in plant-insect interaction (Lan *et al.* 2014). Plant aspartyl proteases are an integral part of the plant immunity and play imperative role in plant-pathogen interaction (Figueiredo *et al* 2021). The DELs forming a competing network with miRNAs and DEGs that possess great significance in plant-insect interaction clearly indicates the involvement of these DELs in tea plant's response to TMB infestation.

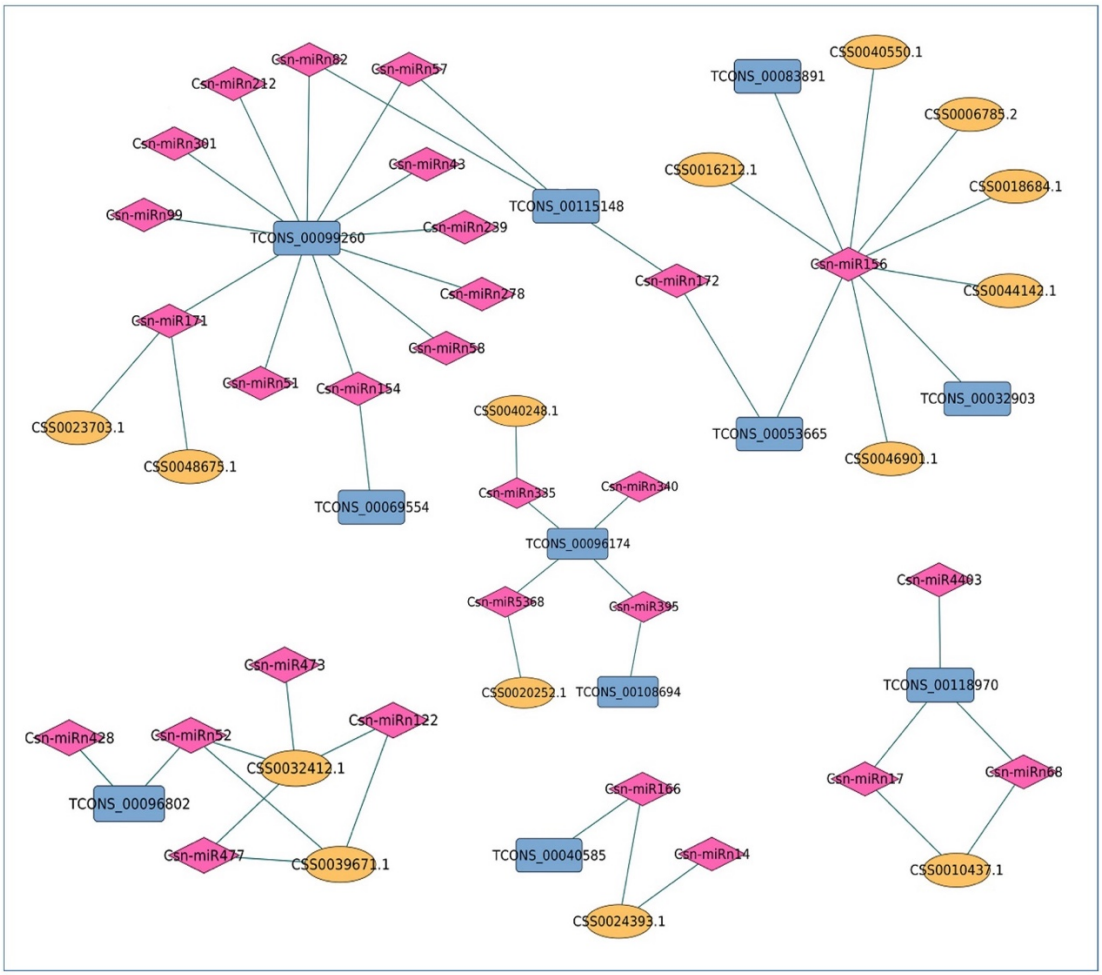

Fig. 4.40 TMB-responsive miRNA-lncRNA-mRNA network in *C. sinensis*. miRNAs, mRNAs and lncRNAs are represented by pink prismatic shape, yellow ellipse and blue round rectangles respectively. The interactions between the RNA molecules are depicted by blue edges.

```
>csn-miR172g-3p Score: 2.5      CSS0016124.1

Query:          1 AGAATCTTGATGATGCTGCATG 22
                  |||||||:|||||*||||**||
Sbjct:        449 TCTTAGAGCTACTTCGACCAAC 428


>csn-miR172g-3p Score: 1.2      CSS0037440.1

Query:          1 AGAATCTTGATGATGCTGCATG 22
                  ||||||:|||||||||||||*:|
Sbjct:       1330 TCTTAGGACTACTACGACG-GC 1310


>csn-miR1310a   Score: 2.5      CSS0028947.1

Query:          1 AACTTTAAATAGGTAGG 17
                  |||||:||||||*|||*
Sbjct:        698 TTGAAGTTTATCAATCG 682


>csn-miR1310a   Score: 2.5      CSS0030458.1

Query:          1 AACTTTAAATAGGTAGG 17
                  |||:||*|*||||||||
Sbjct:       1342 TTGGAAATAATCCATCC 1326
```

Fig. 4.41 miRNA targeting mRNA analysis through psRobot_tar; Score depicts the expectation threshold; Query determines the miRNA and subject determines the mRNA; Asterisks (*) determine unpaired regions.

To predict whether the *C. sinensis* miRNAs had any binding affinity with the identified DECs, we searched for the sequence complementarity between *C. sinensis* miRNAs and DECs. A total of 17 DECs were predicted to be potential targets for 55 *C. sinensis* miRNAs. These 17 DECs were also assessed for their potential to act as miRNA sponges. The DECs were found to be eTMs of 9 DEGs. The DEC Csi_circRNA_282 has been predicted to mimic 3 DEGs (CSS0022312.1, CSS0030486.1 and CSS0007153.1), two of which code for the enzyme phospholipase and the third one codes for a lectin-receptor like kinase (LecRLK). Another DEC Csi_circRNA_219 has been found to be a decoy of 3 genes (CSS0040248.1, CSS0043875.1 and CSS0012190.2) coding for enzymes aspartyl protease and tropinone reductase. Other genes potentially mimicked by identified DECs include condensin complex subunit (CSS0013476.1) and DNA helicase

(CSS0007026.1). Fig. 4.42 depicts the miRNA-circRNA-mRNA interaction network. Three types of interactions are observed in the network (a) a single circRNA acting as a target for a single miRNA (b) a single circRNA acting as a target for more than one miRNA (c) genes and circRNAs acting as common miRNA targets. From the network visualization, it is evident that tea plant circRNAs might play inevitable role in regulation of gene expression by acting as common miRNA targets or miRNA sponges.

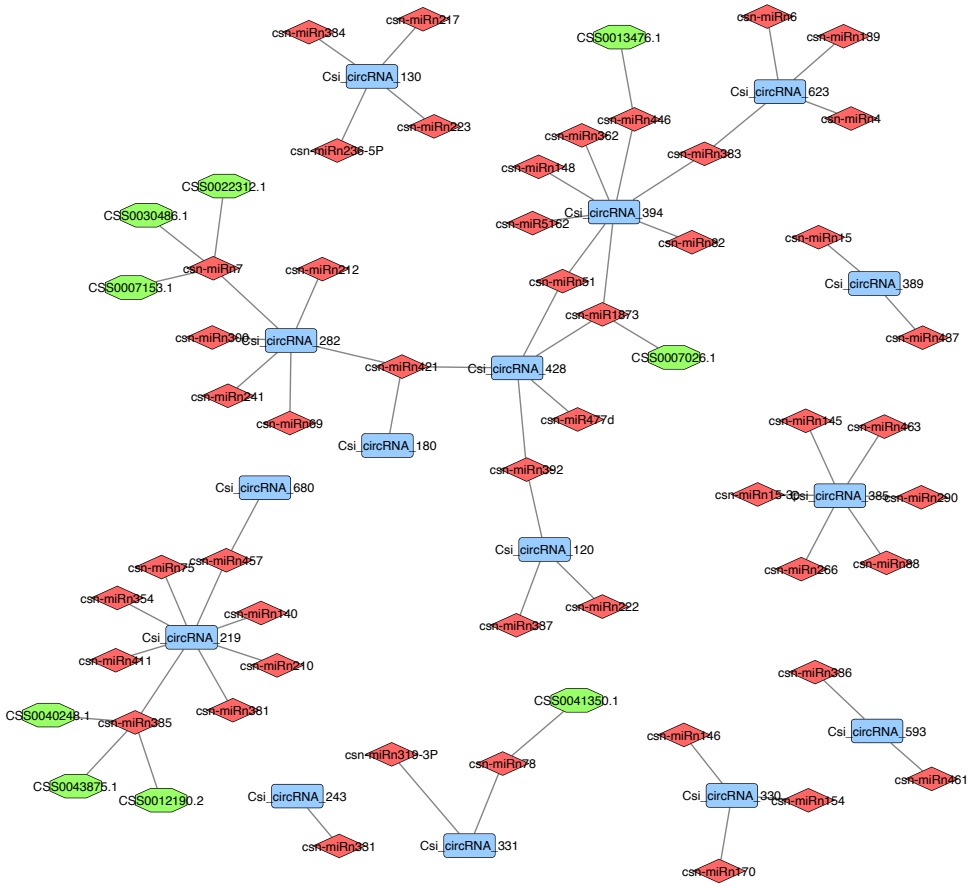

Fig. 4.42 *C. sinensis* miRNA-DEC-DEG interaction network. miRNAs, genes and circRNAs are represented by red diamonds, green octagons and blue rectangles respectively. The connections between the RNA molecules are depicted by black edges.

Table 4.8 List of DECs being targeted by *C. sinensis* miRNAs

miRNA	Target	E-value	miRNA_start	miRNA_end	Target_start	Target_end	miRNA_aligned_fragment	Target_aligned_fragment	Inhibition
csn-miRn222	Chr11:34838916-34896102	1.5	1	24	4414	4437	AUCCGAUAGACAUGAUUUUUACA	UAUAAAAAAUCACGUCUAUCGGAU	Cleavage
csn-miRn337	Chr11:34838916-34896102	2	1	24	5246	5269	AAAUAUAAACCUCAAGGGACGAGA	AUUUACCCCCUGAGGUUUAUAUUU	Cleavage
csn-miRn392	Chr11:34838916-34896102	2	1	24	38689	38712	UUUAGAAAGAGAAAUAGAAAAGGU	UUUCCUUUUAUUUUUUUUUCUGAA	Cleavage
csn-miRn392	Chr11:34838916-34896102	2	1	24	8662	8685	UUUAGAAAGAGAAAUAGAAAAGGU	UUUCCUUUUAUUUUUUUUUCUGAA	Cleavage
csn-miRn58	Chr11:59408657-59454641	0.5	1	24	40510	40533	AUGGACCAAAUUGACACAUCAUGU	ACACAAUGUGUCAAUUUGGUCUAU	Cleavage
csn-miRn334	Chr11:59408657-59454641	1	1	24	40501	40524	AUUGACACAUUGUAUAAACUACAA	CAAUAGUUUACACAAUGUGUCAAU	Cleavage
csn-miRn236	Chr11:59408657-59454641	1.5	1	24	40863	40886	AUACGAUGUGUCAAUUUGGUACCU	AGUGACCAAAUUGAUACAUUGUGU	Cleavage
csn-miRn217	Chr11:59408657-59454641	2	1	24	40501	40524	AUUGACACAUUGUUUAACCUUCCG	CAAUAGUUUACACAAUGUGUCAAU	Cleavage
csn-miRn223	Chr11:59408657-59454641	2	1	24	40512	40535	AUAGAGACCAAAUUGACACAUUGU	ACAAUGUGUCAAUUUGGUCUAUGU	Cleavage
csn-miR168a	Chr12:11978061 3-119784161	0	1	21	3467	3487	CCCGCCUUGCAUCAACUGAAU	AUUCAGUUGAUGCAAGGCGGG	Cleavage

csn-miR168a	Chr12:119780613-119784161	0	1	22	3466	3487	CCCGCCUUGCAUCAACUGAAUU	GAUUCAGUUGAUGCAAGGCGGG	Cleavage
csn-miR168c	Chr12:119780613-119784161	1	1	21	3467	3487	CCCGCCUUGCAUCAACCGAAU	AUUCAGUUGAUGCAAGGCGGG	Cleavage
csn-miRn421	Chr13:101785941-101800633	2	1	24	3085	3108	UUUAGAAAGGAAAAGAAAAAAGAU	UCUUUUUUUUUUUUUUUUUUUAAA	Cleavage
csn-miRn210	Chr13:95736514-95828107	1	1	24	50388	50411	UGAACAAGUUACAGUUAUUGGAUU	GAUCCGAUAACUGUAACUUGUUUA	Cleavage
csn-miRn140	Chr13:95736514-95828107	1.5	1	24	73273	73296	UGGUCAUGGAAGCAACAAAACAAG	UGCCAUUUGAUGCUUCCAUGAUCA	Cleavage
csn-miRn335	Chr13:95736514-95828107	2	1	24	34772	34795	GAAAGGAAAAUGAAAAAAGUAGGU	AUGUUAUUUUUUCAUUUUUUUUUC	Cleavage
csn-miRn354	Chr13:95736514-95828107	2	1	24	50383	50406	AAGUUAUAAUUAUCGGAUCAGCCU	AGGUCGAUCCGAUAACUGUAACUU	Cleavage
csn-miRn381	Chr13:95736514-95828107	2	1	25	43372	43396	AAUAAUCAUGAAAGAUUUGUGAUCA	AUAAAGCAAAUGUUUCAUGAUUAUG	Cleavage
csn-miRn411	Chr13:95736514-95828107	2	1	23	13157	13179	AAGAGAUUUGGAAAGGAAAACGG	UUCUUUAUCUUUUCAAAUCUCUU	Cleavage
csn-miRn457	Chr13:95736514-95828107	2	1	24	69982	70005	AUACUAAUUAGUGCAUGUAGUACC	GAUACUACAUGCACCAAUUAGUGU	Translation
csn-miRn75	Chr13:95736514-95828107	2	1	24	50387	50410	AAACAAGUUACAAUUGUCGGACCC	CGAUCCGAUAACUGUAACUUGUUU	Cleavage
csn-miRn331	Chr14:49644209-49664819	2	1	24	17466	17489	AUGAUCAUGAAAGAUUUGUAACCU	UAUGGACUAAGCUUUCAUGAUCAU	Cleavage

csn-miRn241	Chr15:36236089-36288888	1	1	24	9473	9496	AUUGAUCGGAUAUCGAUAGUAACU	AAUAGUUAUCGAUAUCUGAUCAAU	Cleavage
csn-miRn7	Chr15:36236089-36288888	1	1	24	44390	44413	AAAUUCUUGAACCAAAUGCAGCCU	AGGCUGUAUUUGGUUCAAGGAUUU	Cleavage
csn-miRn212	Chr15:36236089-36288888	1.5	1	24	8030	8053	UUGGAAAAGGAAAGGGAAAAUGUC	UUUUUUUUCCCUUUUUUUUUUCAA	Cleavage
csn-miRn300	Chr15:36236089-36288888	1.5	1	25	9386	9410	CUGAUUUGAUCACAUAGCUAUUGAA	ACCGAUAGCUAUGUGAUCAAAUGAG	Cleavage
csn-miRn69	Chr15:36236089-36288888	1.5	1	24	6489	6512	GUUUGGCUGGAGGAUUUGGAAAAG	CCUCCCCAAAUCCUCCAACCAAAC	Cleavage
csn-miRn421	Chr15:36236089-36288888	2	1	24	41659	41682	UUUAGAAAGGAAAAGAAAAAAGAU	AGCAUUUUUUUUUUCUUUUUUAGA	Cleavage
csn-miRn241	Chr2:28206828-28300807	0	1	24	75479	75502	AUUGAUCGGAUAUCGAUAGUAACU	GAUAGCUAUCGAUAUCCGAUCAAU	Cleavage
csn-miRn170	Chr2:28206828-28300807	1	1	24	75485	75508	AAUCAUAUUGAUCGGAUACCAAUA	UAUCGAUAUCCGAUCAAUAUGAUU	Cleavage
csn-miRn146	Chr2:28206828-28300807	1.5	1	24	14028	14051	AAGAGAUUUAGAAAAGAAAAAGAA	AUAUAUAUCUUUUUUAAAUCUCUU	Cleavage
csn-miRn154	Chr2:28206828-28300807	1.5	1	24	66749	66772	UUUGAAAAGGGAAAUGGAAAACAU	UACGUUUGCAUUUCCCUUUUUAAA	Cleavage
csn-miRn124	Chr2:30957568-30972440	0	1	24	11101	11124	UAAAAUUGACUGAUCAGUUAGACU	AGCCUAACUGAUCAGUCAAUUUUA	Cleavage
csn-miRn319	Chr2:30957568-30972440	2	1	24	8531	8554	AUUCAGAAUGAUGUGGCAAUGGUA	CUCCCUUGCCACAUCAUUAUGAGU	Cleavage

csn-miRn78	Chr2:30957568-30972440	2	1	24	7309	7332	AAUUCGAGCCAUUUGAACCACAGA	ACAUAGGUUCCAGUGGCUCGAGUU	Cleavage
csn-miRn290	Chr3:24712125-24723830	0.5	1	24	3910	3933	AUGUGUAAAAAGUGUAUUAAAAUA	AAUUUUAAUAUACUUUUUACACAU	Cleavage
csn-miRn145	Chr3:24712125-24723830	1.5	1	24	10345	10368	AUGUUAGAGGACCACAAUUUUUGU	ACAAAAAUUGUGGUCCUCAAACAU	Cleavage
csn-miRn266	Chr3:24712125-24723830	1.5	1	24	10346	10369	AAUGUUUGAGGGCCACAAAAUCAG	CAAAAAUUGUGGUCCUCAAACAUU	Cleavage
csn-miRn290	Chr3:24712125-24723830	1.5	1	24	7838	7861	AUGUGUAAAAAGUGUAUUAAAAUA	AAUUUUAAUAUAUUUUUUAUACAU	Cleavage
csn-miRn88	Chr3:24712125-24723830	1.5	1	24	7501	7524	UACACUAAUUGAUACAUGUAGCCU	GUACUACAUGUAUCAAUUAGUAUA	Cleavage
csn-miRn15-	Chr3:24712125-24723830	2	1	21	1216	1236	UGAAUGGUAUGAAUCACUUUG	AAAAUUGAUUUAUACCAUUUA	Cleavage
csn-miRn463	Chr3:24712125-24723830	2	1	24	10227	10250	ACAAAAAUUGUGGCACUCAAACAU	AUGCUAGAGGGCCACAAUUUUUGU	Cleavage
csn-miRn15	Chr3:28928697-28958380	2	1	24	9249	9272	AUACUUGGUAGCUCGAAUUUGUGU	UGCUCAACCCGAGCUACCAAGUAU	Cleavage
csn-miRn437	Chr3:28928697-28958380	2	1	24	8605	8628	AUGAAUGGUGUAGAUCAGUAAGGG	GAAUCAUUCAUCUACACUAUUCAU	Cleavage
csn-miRn471	Chr3:32458632-32484366	0.5	1	24	5445	5468	AAAGAAAAUGAGAUAUCCGUGCCU	AGGCACGGAUAUCUCGUUUUCUUU	Cleavage
csn-miR1873	Chr3:32483405-32623875	1	1	20	127609	127628	UGGCUCUGAUACCAUGUUGA	UUAACAUGGUAUCAGAGCCG	Cleavage

csn-miRn51	Chr3:32483405-32623875	1.5	1	24	106234	106257	AGUGAUUUGGAAAACGAAAGAGAA	UUCUCUUUCUUUUUUCAAAUCACU	Cleavage
csn-miRn82	Chr3:32483405-32623875	1.5	1	24	55141	55164	UUUGGAAAGAGAAAAGAAAAAGAC	CAACGAUUUUUUUCUCUUUCCAAA	Cleavage
csn-miR5162	Chr3:32483405-32623875	2	1	24	22898	22921	AUGACCAAAAUACCCCUAGAACAU	AAGUGUUAGGGGUAUUUUGGUCUU	Cleavage
csn-miRn148	Chr3:32483405-32623875	2	1	24	106240	106263	UUGAGAAGCGAUUUGGAAAGAGAA	UUCUUUUUUCAAAUCACUUCUCAA	Cleavage
csn-miRn362	Chr3:32483405-32623875	2	1	24	23861	23884	UUCGGAAAUUACAGAUACCCUCCU	CAAGGGGUAUUUGUAAUUUCCCAA	Cleavage
csn-miRn383	Chr3:32483405-32623875	2	1	24	23863	23886	AUUUGAGAAAUUACAGAUACUCCC	AGGGGUAUUUGUAAUUUCCCAAAU	Cleavage
csn-miRn446	Chr3:32483405-32623875	2	1	24	33608	33631	AGAAGAGAAUGUAUUUGAAACAAA	CAAAUUUCAAAUAUCUUCUCUUCU	Translation
csn-miRn51	Chr3:32483405-32623875	2	1	24	127607	127630	AAUGGCUCUGAUACCAUGUUGAAA	AUUUAACAUGGUAUCAGAGCCGGU	Cleavage
csn-miRn51	Chr4:161368403-161435297	1	1	24	44025	44048	AAUGGCUCUGAUACCAUGUUGAAA	AACUUACAUGGUAUCAGAGCCAUC	Cleavage
csn-miRn392	Chr4:161368403-161435297	1.5	1	24	20785	20808	UUUAGAAAGAGAAAUAGAAAAGGU	AAACUUUCUCUUUUUCUUUCUAAA	Cleavage
csn-miRn421	Chr4:161368403-161435297	1.5	1	24	20785	20808	UUUAGAAAGGAAAAGAAAAAAGAU	AAACUUUCUCUUUUUCUUUCUAAA	Cleavage
csn-miR1873	Chr4:161368403-161435297	2	1	20	44027	44046	UGGCUCUGAUACCAUGUUGA	CUUACAUGGUAUCAGAGCCA	Cleavage

csn-miR477d	Chr4:161368403-161435297	2	1	20	56331	56350	AAAGGCUUCCAAUAUUCUAU	GCAGAAUGUUGGAAGCUUUU	Cleavage
csn-miRn336	Chr8:37959648-37979650	1.5	1	24	9506	9529	AUGACCCUUGGAUUACACUUAGAA	UUCUAAGUGUAAUCCAAGGGUUAC	Cleavage
csn-miRn461	Chr8:37959648-37979650	2	1	24	9511	9534	GUUUUGUGACCCUUGAAUUACACU	AGUGUAAUCCAAGGGUUACAAAGC	Cleavage
csn-miRn383	Chr9:15929212-15985356	1.5	1	24	3484	3507	AUUUGAGAAAUUACAGAUACUCCC	AAUAAAAUCUGUGAUUUCUCAAAU	Cleavage
csn-miRn4	Chr9:15929212-15985356	1.5	1	21	17810	17830	UCUCUUCUAUAUAUAGGCAUC	GAUUCCUAUAUAUAGAAGAGG	Cleavage
csn-miRn4	Chr9:15929212-15985356	1.5	1	21	20605	20625	UCUCUUCUAUAUAUAGGCAUC	GAUUCCUAUAUAUAGAAGAGG	Cleavage
csn-miRn6	Chr9:15929212-15985356	1.5	1	21	17810	17830	UCUCUUCUAUAUAUAGGCAUC	GAUUCCUAUAUAUAGAAGAGG	Cleavage
csn-miRn6	Chr9:15929212-15985356	1.5	1	21	20605	20625	UCUCUUCUAUAUAUAGGCAUC	GAUUCCUAUAUAUAGAAGAGG	Cleavage
csn-miRn139	Chr9:15929212-15985356	2	1	24	791	814	AGAAAAUUUGGUGUCUCUAACAUU	AAUGUUAGGGAUAUCAAAUUUUUU	Cleavage
csn-miRn457	Contig426:218590-239885	2	1	24	3459	3482	AUACUAAUUAGUGCAUGUAGUACC	ACUAGUAUGUGCACUAAUUAGUAC	Cleavage

4.8 ceRNA network

To have a complete overview of the interaction between genes and ncRNAs during tea-TMB communication, construction of a ceRNA network involving mRNAs, miRNAs, lncRNAs and circRNAs was done in order to reflect an overall picture of the ceRNA network. The ceRNA network included 5 lncRNAs, 17 circRNAs, 33 mRNAs and 37 miRNAs.

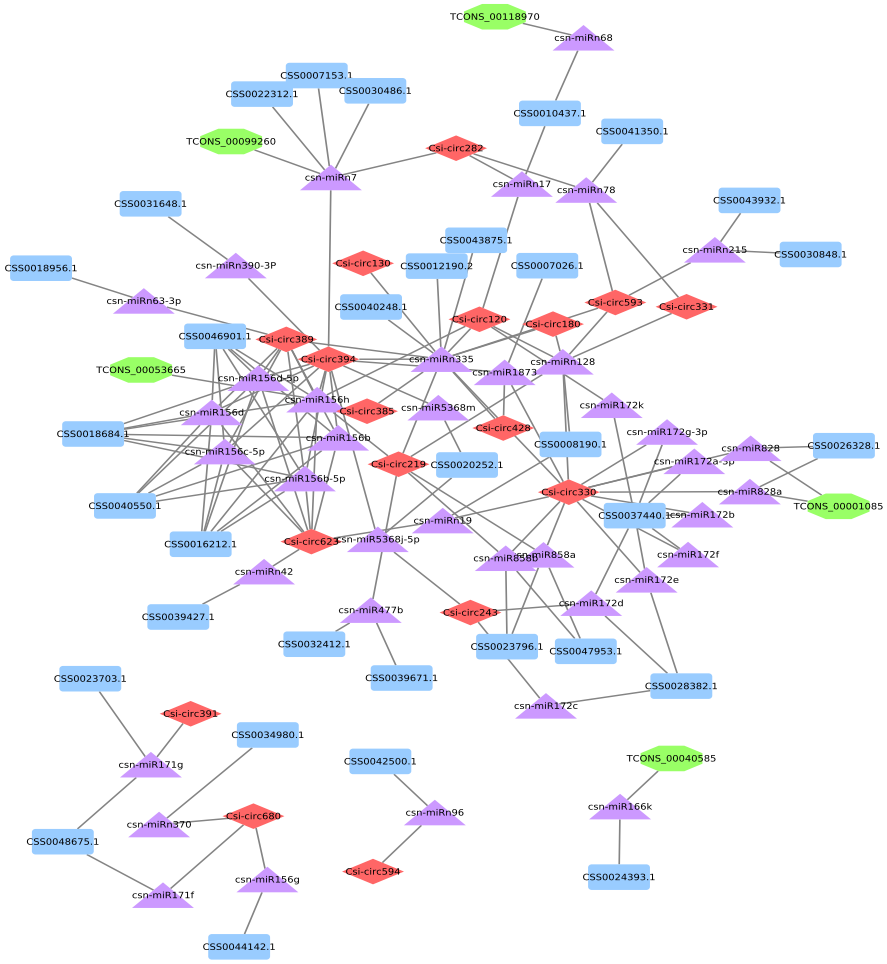

Fig. 4.43 TMB-responsive ceRNA network in *C. sinensis*. miRNAs, mRNAs, lncRNAs and circRNAs are represented by purple prismatic shape, blue round rectangles, green octagons and red diamonds respectively. The interactions between the RNA molecules are depicted by black edges.